الجمهورية الجزائرية الديموقراطية الشعبية
République Algérienne Démocratique et Populaire
وزارة التعليم العالي و البحث العلمي
Ministère de L'Enseignement Supérieur et de la Recherche Scientifique

ÉCOLE NATIONALE POLYTECHNIQUE D'ALGER
Département du Génie des Procédés et Environnement

End of studies project thesis

Presented with a view to obtain the diploma of state engineer

In process and environmental engineering

Demineralization of treated wastewater by electrodialysis coupled with resins to be used as medium-pressure BFW

Ms. HANNACHE Lyna and Ms. SAYOUD Besma

Publicly presented and defended on the 6^{th} of July 2023.

Jury members:

Mrs.	Bensadellah Leila	Associate professor	ENP	President
Mr.	Belkadi Mohammed El Amin	Head of service ETP	Sonatrach	Director thesis
Mr.	Mameri Nabil	Professor	ENP	Co-director thesis
Mr.	Mazighi Ahmed	Professor	ENP	Examinator
Mr.	Kherat Mohamed	Ph.D. student	ENP	Guest

ENP 2023

الجمهورية الجزائرية الديموقراطية الشعبية
République Algérienne Démocratique et Populaire
وزارة التعليم العالي و البحث العلمي
Ministère de L'Enseignement Supérieur et de la Recherche Scientifique

ÉCOLE NATIONALE POLYTECHNIQUE D'ALGER
Département du Génie des Procédés et Environnement

End of studies project thesis

Presented with a view to obtain the diploma of state engineer

In process and environmental engineering

Demineralization of treated wastewater by electrodialysis coupled with resins to be used as medium-pressure BFW

Ms. HANNACHE Lyna and Ms. SAYOUD Besma

Publicly presented and defended on the 6^{th} of July 2023.

Jury members:

Mrs.	Bensadellah Leila	Associate professor	ENP	President
Mr.	Belkadi Mohammed Amin	Head of service ETP	Sonatrach	Director thesis
Mr.	Mameri Nabil	Professor	ENP	Co-director thesis
Mr.	Mazighi Ahmed	Professor	ENP	Examinator
Mr.	Kherat Mohamed	Ph.D. student	ENP	Guest

ENP 2023

الجمهورية الجزائرية الديموقراطية الشعبية
République Algérienne Démocratique et Populaire
وزارة التعليم العالي و البحث العلمي
Ministère de L'Enseignement Supérieur et de la Recherche Scientifique

ÉCOLE NATIONALE POLYTECHNIQUE D'ALGER
Département du Génie des Procédés et Environnement

Mémoire de projet fin d'études

En vue d'obtention du diplôme d'Ingénieur d'État en Génie des Procédés et Environnement

Déminéralisation des effluents industriels traités par électrodialyse couplé aux résines échangeuses d'ions pour l'alimentation des chaudières à moyennes pression

Mlle. HANNACHE Lyna and Mlle. SAYOUD Besma

Soutenu publiquement, le 06/07/2023, devant le jury composé de :

Mme.	Bensadellah Leila	Professeur	ENP	Président
M.	Belkadi Mohammed Amin	Chef de service ETP	Sonatrach	Directeur de thèse
M.	Mameri Nabil	Professeur	ENP	Co-directeur de thèse
M.	Mazighi Ahmed	Professeur	ENP	Examinateur

ENP 2023

ملخص

يركز هذا العمل على إزالة المعادن من مياه الصرف الصحي المعالجة من مصفاة الجزائر لإعادة استخدامها في غلايات الضغط المتوسط. الطريقة الرئيسية المستخدمة هي التحليل الكهربائي إلى جانب الراتنجات. تم تطوير ديونيزر كهربائي شبه تجريبي لدراسة كفاءة العمليتين. وتوفر نتائج الدراسة معلومات عن أدائها، مما يسهم في ممارسات الإدارة المستدامة للمياه.

الكلمات المفتاحية: إزالة المعادن، استصلاح مياه الصرف الصحي، التحليل الكهربائي، راتنجات التبادل الأيوني.

Résumé

Ce travail se concentre sur la déminéralisation des eaux usées traitées de la raffinerie d'Alger en vue de leur réutilisation dans les chaudières à moyenne pression. Le principal process utilisé est l'électrodialyse couplée aux résines. Un électro-déioniseur semi-pilote a été développé pour étudier l'efficacité des deux processus. Les résultats de l'étude fournissent des informations sur leurs performances, contribuant ainsi aux pratiques durables de gestion de l'eau.

Mots Clée : Déminéralisation, valorisation des eaux usées, électrodialyse, résines échangeuses d'ions.

Abstract

This work focuses on demineralizing treated wastewater from Algiers refinery for reuse in medium pressure boilers. The main method employed is electrodialysis coupled to resins. A semi-pilot electrodeionizer was developed to study the efficacy of both processes. The study's findings provide insights into their performance, contributing to sustainable water management practices.

Keywords: Demineralization, wastewater reclamation, electrodialysis, ion exchange resins.

"This work is dedicated to my beloved family, both big and small"

- Besma

"To the ones I love most and live for, my dear family "

- Lyna

Acknowledgments

First and foremost, we would like to express our sincere gratitude to god who have guided us throughout this journey and allowed us to successfully complete this work, achieving the best possible conditions and results.

We extend our heartfelt appreciation to Sonatrach, with special thanks to ***Mr. Amine Belkadi***, the Head of the Effluent Treatment Plant at Algiers Refinery, for his invaluable supervision and guidance during the three-month period. His constant encouragement and support have been instrumental in the success of this thesis.

We would also like to acknowledge the entire team at the Environmental Laboratory, including ***Mr. Youcef Rechidi, Farida, Roufiada, Bougara, and Zineddine***. Their contributions, expertise, and collaboration have greatly enriched our research and played a significant role in its completion.

We would like to express our deep appreciation and sincere gratitude to our esteemed professor, ***Mr. Nabil Mameri***, for his exceptional guidance and leadership throughout this thesis. We are truly grateful for the time he has dedicated to overseeing this project.

We extend our heartfelt thanks to Miss ***Dr. Leila Bensadallah***, who has honored us by presiding over the thesis defense committee. We would also like to express our gratitude to ***Pr. Ahmed Mazighi*** for accepting the role of examinator.

Special thanks are extended to ***Dr. Mohamed Kherrat***, who accompanied us in the laboratory, helping us solving technical challenges and providing support throughout the research process. We are grateful for his presence as an invited member of the jury.

We acknowledge the immense contributions of all the members of the thesis defense committee, and we sincerely thank them for their time, expertise, and valuable insights.

Contents

List of Figures

List of Tables

Nomenclature

Acronymes

AEM	Anion Exchange Membranes
BFW	Boiler Feed Water
BOD	Biochemical Oxygen Demand
CaH	Calcium Hardness
CDEI	Continuous electrodeionization
CEM	Cation Exchange Membrane
COD	Chemical Oxygen Demand
DOC	Dissolved organic carbon
DW	Distillated water
ED	Electrodialysis
EDI	Electrodeionization
FAO	Fodd and Agriculture organisation
GAC	Granulated Activated Carbon
I_{lim}	Limiting current density
IEM	Ion exchange Membranes
IXR	Ion exchange resin
IXR	Ion exchange resins
LPG	Liquified petroleum gas

PCB	polychlorinated biphenyls
q	Adsorption density
TAT	Total Alkalinity Title
TH	Total hardness
THM	trihalomethanes
TN	Total Nitrogen
TOC	Total organic Carbon
TSS	Total Suspended Solids
WW	Wastewater
ZLD	Zero Liquid Discharge

General Introduction

Water is a precious resource that is essential to sustain life on earth. It is vital for various purposes such as agriculture, transportation, sanitation, and energy production. However, the growing demand for freshwater resources has resulted in the depletion of this essential resource. The increasing population and industrialization have contributed to water pollution, further reducing the availability of freshwater resources. The consequences of water scarcity are significant, affecting both the environment and human society. The effects of droughts, reduced crop yields, and decreased access to safe drinking water have far-reaching consequences. It impacts various sectors such as agriculture, energy, and industry, leading to economic losses and societal upheaval. In response to the challenges posed by water scarcity, many industries are seeking alternative sources of water to meet their needs. Water recycling and reclamation technologies have become increasingly popular, allowing industries to reuse wastewater and other non-traditional sources of water.

One application of treated wastewater is BFW for medium pressure boilers. These boilers are used in many industries, including power generation, petrochemical, pulp and paper; they require high-quality water to prevent mineral deposition and corrosion, which can reduce the efficiency and lifespan of the boiler. Using treated wastewater as feedwater for medium pressure boilers can provide a sustainable and cost-effective alternative to freshwater sources.

However, treated wastewater contains high levels of dissolved minerals, such as calcium, magnesium, and silica, which can cause scaling and corrosion in high-pressure boilers. Therefore, the demineralization of treated wastewater is necessary to achieve the required water quality for high-pressure boilers.

The demineralization of treated wastewater involves the removal of dissolved minerals using various technologies and processes. These technologies include ion exchange, reverse osmosis, electrodialysis, and others. Each technology has its advantages and limitations, and the selection of the appropriate technology depends on several factors, such as the water quality requirements, the composition of the treated wastewater, and the economic feasibility.

In recent years, there has been a growing interest in the demineralization of treated wastewater for high-pressure boilers, and several studies have been conducted to investigate the feasibility and effectiveness of different demineralization technologies and processes. However, there is still a need for further research to optimize the demineralization process, reduce costs, and minimize the environmental impact.

The main purpose of this work, is to investigate the performance comparison between a lab-scale electro-deionizer (EDI) and a conventional electrodialysis coupled with resins, in order to assess the efficacy and potential advantages of the EDI technology for water

deionization. The research will focus on optimizing the operating conditions of the electrodialysis-ion exchange process to achieve the desired level of demineralization while minimizing the energy consumption and other costs associated with the process. The thesis will begin with an overview of the current state of water resources in Algeria and the need for sustainable alternatives. This will be followed by a literature review that will explore the different demineralization technologies and processes that can be used for treating wastewater as well as the pre-treatment techniques that come upstream of the electrodialysis including filtration on a bed granulated with activated charcoal.

The research will involve laboratory-scale experiments to investigate the effect of various parameters on the efficiency of the electrodialysis-ion exchange process. These parameters include the feed water composition, the applied electric field, the ion-exchange resin type, and the operating pH. The quality of the treated water will be evaluated at first using various analytical techniques, the said characterization shall encompass the calculation of relevant parameters such as suspended matter, chemical oxygen demand, and biological oxygen demand.

Finally, the thesis will conclude with a discussion of the main findings and implications of this work, as well as recommendations for future research and practical applications of the research outcomes. This work will contribute to the development of sustainable and cost-effective solutions for the use of treated wastewater as feedwater for medium pressure boilers, and thus help to alleviate the pressure on freshwater resources.

Part I

Literature Review

Chapter 1

Wastewater Reclamation in Refineries: An Overview

1.1 Introduction

The refining industry is a major water consumer, using various sources of water.

Wastewater reclamation has become crucial as environmental regulations increase, with refineries developing techniques for treating and reclaiming it. However, over 80% of all wastewater produced is discharged into the environment without adequate treatment [1].

The present chapter will begin by discussing the potential significance and innovation of the research. Then, it will present the different advanced treatment processes, used for the treatment of wastewater in Algiers Refinery. Finally, the chapter will highlight the potential applications of the treated wastewater in the refinery, including its use as a source of water for high-pressure boilers.

1.2 The study context

1.2.1 The thesis objectives

In fact, according to the Food and Agriculture organisation (FAO), out of 180 countries, Algeria is classified among the 17 countries with the poorest water potential. With only 478 m^3/person/year of renewable water, it has less than 50% of the scarcity threshold set by the World Bank at 1000 m^3/person/year and less than 33% of the water comfort threshold set between 1000 and 1700 m^3/person/year (FAO, 2003). As depicted in Figure 1.1, illustrating projected water stress by country for the year 2040, it is evident that Algeria's water withdrawals for supply are expected to exceed 80%, which raises concerns. Thus, it became mandatory to prioritise high-quality water for drinking and using reclaimed water for lower-risk applications like irrigation and industrial feeds [2].

One aspect of this is reusing water as feed for boilers, which represents a technical and economic challenge due to the typically low quality of the source water required and the high quality needed to sustain the boilers.

1.2.2 The internship site

The Algiers Refinery was established in December 1959, subsequent to the discovery of oil in southern Algeria. Construction began in January 1960, and the facility was inaugurated on January 19th 1964 by a consortium of foreign companies, including Shell, ESSO Mediterranean, and Total S.A.H.M

The refinery, covering an area of 182 hectares, is situated 20 km east of Algiers. Following rehabilitation, the refinery's crude oil, coming from Hassi-Messaoud, processing

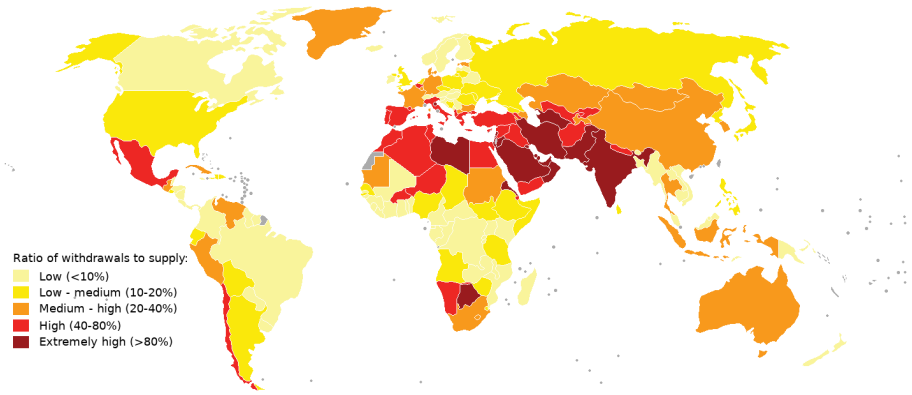

Figure 1.1: Water stress by country by year 2024 (Word Ressources Institue, 2018)

capacity increased from 2.7 to 3.5 million tons per year. The main products of the facility are diesel, premium gasoline, and kerosene, with annual production capacities of 1,261,667 tonnes, 757,000 tonnes, and 620,666 tonnes, respectively.

The processing units at the refinery include a crude distillation unit, a fluid catalytic cracking unit, a hydrocracker unit, a reformer unit, and other units for producing various products such as gasoline, diesel fuel, jet fuel, and Liquified Petroleum Gas (LPG). The refinery's products are transported via pipelines, ships, and trucks to various destinations in Algeria and beyond.

The refinery, being a significant entity in petrochemical refining, prioritizes the conservation of the environment. To this end, it has implemented specific measures to manage the various types of wastes generated during its operations, such as the Effluent Treatment Plant. [3].

1.3 Treatment processes of wastewater in Algiers refinery

1.3.1 Origin of effluents

- **Runoff water potentially contaminated with hydrocarbons**
- **Effluents continuously polluted with hydrocarbons:** Acidic stripping water.
  Brine from the crude distillation unit.
  Purge water from crude oil tanks and recovery products.
  Used caustic.
- **Effluents not contaminated with hydrocarbons:** Purge from the cooling water and boiler circuit.

Neutralized effluents from the demineralization unit.
Gravity sewer for non-polluted water.

1.3.2 Process description of new effluent unit plant 850

1. **Rainwater tank**: They collect water in case of storms or when the flow exceeds 200 m^3, equipped with three 24-inch manholes and 3 skimming plates that allow the removal of oils and polluted sludge.

2. **Waste caustic soda equalization tank**: The waste caustic soda is injected into or before the equalization tank using a pump at a flow rate of 350 l/h. pH correction with sulfuric acid can be done by pump to balance and neutralize the deoiled effluent.

3. **Circular DCI separation:** A gravity separator between water, solid and insoluble oil. It operates in laminar flow without effluent equalization.

4. **Equalization tank:** The deoiled water from the DCI unit, and rainwater reservoir are received in the equalization tank to thoroughly mix the water and maintain constant hydraulic and mass loads.

5. **DAF (Dissolved Air Flotation)**: An equipment used for the separation of solid particles, fats, and oils that have not been removed by the DCI separator. Gas is introduced to form tiny gas bubbles that adhere to the incoming matter, causing it to rise to the surface. DAF incorporates a stable feed with coagulation-flocculation operation, flotation, and pressurization system.

6. **Biological treatment:** The unit is fed with treated water from the DAF unit and microorganism nutrients (H3PO4 and urea), with recirculation of sludge from the clarifier. The basin is working on mode extended aeration, operating with low-loaded activated sludge where bacteria undergo self-oxidation (endogenous respiration).

7. **Sand filtration with FLA (Fine-Layer Artificial Media):** When the solids load is already low, the VSWF67 filter with 3 autonomous backwashing functions operates in both filtration and backwashing modes independently and automatically, based on a fixed maximum loss value.

8. **Sludge dewatering unit**: The flocculated sludge is introduced into a centrifuge, where the centrifugal force causes the sludge to be propelled at high speed against the walls of the bowl and deposited. The clarified water is removed through the overflow.

1.4 Opportunities for treated wastewater reclamation in Algiers Refinery

Since the 1990s, industries have been subject to increasingly strict environmental regulations, particularly regarding the discharge of wastewater. The ultimate goal is to achieve zero liquid discharge (ZLD), which involves completely eliminating all waste discharges into receiving waters. However, to achieve this goal, industries can use processed or treated wastewater in various industrial applications. Such an approach not only reduces waste discharge but also extracts valuable resources from the wastewater [2].

1.4.1 Reuse of treated wastewater for industrial applications

1.4.1.1 Cooling water systems

Cooling water systems are a major industrial water reuse application and are particularly prevalent among other reuse methods. In certain industries, such as electric power generating stations and oil refining, cooling tower makeup water usage can make up a significant portion of the total water consumption, ranging from one quarter to more than one-half of the total [4]. Power plants frequently employ disinfected secondary effluent for cooling purposes like filtration, chemical precipitation or ion exchange [3]

Key water quality variables include pH, alkalinity, organics, nutrients, and those that affect corrosion and scaling. Typical water quality requirements for cooling water systems versus the boiler feedwater are given in Table 1.1.

Table 1.1: Typical reclaimed water quality requirements for industrial processes

Parameter	Unit	Boiler feedwater			Cooling water	
		Low presssure (<10 bar)	Intermediate pressure (10-50 bar)	High pressure (>50 bar)	Fresh	Brackish
Aluminum	$mg.L^{-1}$	5	0.1	0.01	0.1	-
Ammonia	$mg.L^{-1}$	0.1	0.1	0.1	-	-
Bicarbonate	$mg.L^{-1}$	170	120	48	25	-
Calcium	$mg.L^{-1}$	As received	0.4	0.01	50	420
Chloride	$mg.L^{-1}$	As received	As received	As received	500	-
Copper	$mg.L^{-1}$	0.5	0.05	0.05	0.5	-
Hydrogen sulfide	$mg.L^{-1}$	As received	As received	As received	-	-
Iron	$mg.L^{-1}$	1	0.3	0.05	0.1	-
Manganese	$mg.L^{-1}$	0.3	0.1	0.01	0.5	-
Magnesium	$mg.L^{-1}$	As received	0.25	0.01	-	-
Silica	$mg.L^{-1}$	30	10	0.7	50	25
Sulfate	$mg.L^{-1}$	As received	As received	As received	200	2700
Zinc	$mg.L^{-1}$	0.01	0.01	-	-	-
Alkalinity	$mg.L^{-1}$ as $CaCO_3$	350	100	40	20	115
Chemical oxygen demand	$mg.L^{-1}$	5	5	1	75	75
Dissolved solids	$mg.L^{-1}$	700	500	200	500	35
Suspended solids	$mg.L^{-1}$	100	5	0.5	100	100
Hardness	$mg.L^{-1}$ as $CaCO_3$	350	1	0.07	130	6250
pH	-	7.0-10.0	8.2-10.0	8.2-9.0	-	-
Temperature	C	As received	As received	As received	38	49

1.4.1.2 Boiler Feedwater

Boilers are essential in industrial processes to produce hot water and/or steam for moving turbines and heating materials. Manufacturing plants often require hot water or steam, and thermoelectric plants use combustible energy for generating steam [4].

- **System description** : Boilers can be categorized into three types: fire-tube, water-tube, and electric boilers. A heat source, a water drum, a water inlet, and a steam

outlet are the components of a basic boiler. In this kind of boiler, heat is applied after the water drum is only partially filled. When the water is sufficiently heated, steam begins to form (see Figure 1.2). As the steam exits the vessel, it is captured and sent to additional stages of the process (such as a heat exchanger or a steam turbine to turn a process fluid). Then, makeup water is added to the drum to make up for the liquid that was lost to steam [5].

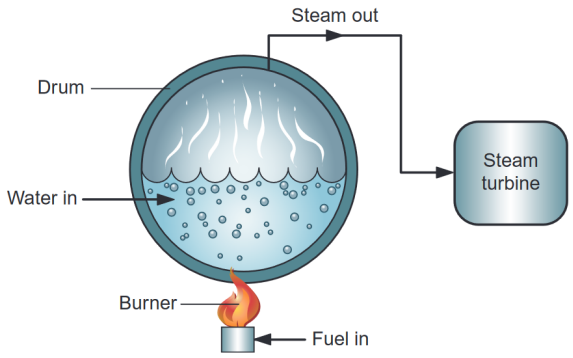

Figure 1.2: Simple boiler

- **Boiler system using reclaimed water**: Figure 3.1 shows a schematic diagram of a boiler system that utilizes reclaimed water. The system includes steam-generating boilers, which produce steam that is used for various applications in the facility. The steam condensate, which is generated during this process, is recycled back to the boiler feedwater due to its low levels of dissolved constituents. However, the amount of condensate generated is often insufficient to meet the feedwater requirements, and as a result, the system requires supplemental makeup water [3].

  In this system, the makeup water is produced from pre-treated and conditioned reclaimed water, which is sourced from a nearby treatment plant. This reclaimed water is treated to remove impurities, such as suspended solids, organic matter, and nutrients, and is then conditioned to meet the required water quality standards for use in the boiler system.

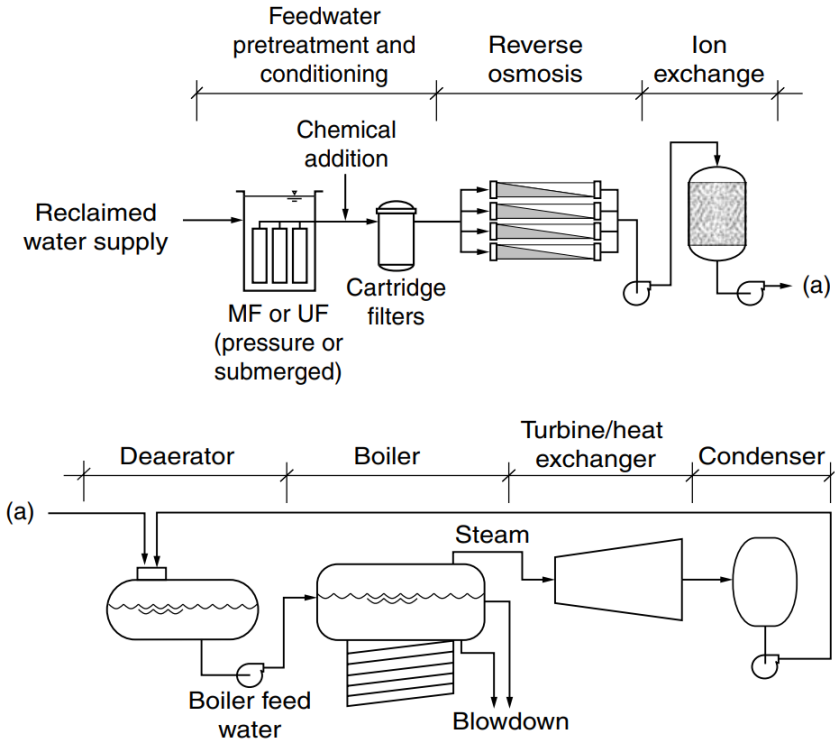

Figure 1.3: Typical flow diagram for a boiler system utilizing reclaimed water

The resulting feedwater, undergoes deaeration to eliminate dissolved oxygen and other gases that could lead to corrosion. The deaerated water is then fed to the boiler system, where it is heated to produce steam.

- **Water quality considerations**: As shown in Table 1.1. displays the recommended quality for boiler feedwater [5]; however, it's important to recognize that specific boiler systems could have their own unique quality standards, which might be more or less strict compared to the suggested values presented in this table.

  Most components of concern in boilers are: [5]

  - pH: If the dissolved solids and pH level are high, the system may be prone to calcium carbonate scaling, which can occur if the pH level goes above 8.2. In many cases, the pH is kept above 7.0 to avoid corrosion issues, but if pH control is not carefully maintained, it can approach the range where calcium carbonate scaling occurs.
  - Alkalinity : Alkalinity indicates the amounts of different ions that can cause problems like foaming and tube overheating in boilers. High alkalinity can result in carbon dioxide content in the steam, leading to corrosion. A balance between too high and too low alkalinity is necessary for protecting

the boiler metal against acidic corrosion while avoiding carry-over conditions. An acidifying agent is commonly injected such as Sulfuric Acid (H_2SO_4) to form soluble salts and lower the pH.

- Silica (SiO_2): Boiler deposits can form due to the presence of silica, which can also vaporize from the boiler and travel with the saturated steam as silicic acid. This vaporized silica can cause insoluble deposits on metal surfaces and critical parts of equipment educing heat transfer efficiency.
- Oxygen: Oxygen can enter the boiler system through various sources, such as water makeup, air leakage, or improper venting. Excessive oxygen levels can lead to corrosion of boiler components, including the metal surfaces and the heat exchanger. Usually the oxygen scavenger is used to remove or reduce the amount of dissolved oxygen present in the boiler water.

1.4.1.3 Process water

Reclaimed water can also be utilized for fire protection purposes, such fire hydrants, landscape irrigation, and in desalter. However, the suitability of reclaimed water for each of these applications depends on the specific water quality there an appropriate treatment process must be implemented to ensure the reclaimed water meets the necessary quality standards [6].

1.4.2 Economic benefits of wastewater valorization

The application of wastewater valorization in refineries offers multiple benefits, including significant cost savings by reducing wastewater treatment and disposal expenses. By recovering valuable resources refineries can create additional revenue streams, decrease reliance on external resources, and enhance overall sustainability. The reclaimed resources can be used internally to lower operational costs, thus improving refinery profitability. Moreover, implementing wastewater valorization helps refineries meet regulatory requirements, enhance their environmental reputation, and gain a competitive edge in the market, leading to long-term profitability [7].

1.5 Conclusion

In conclusion, Algiers Refinery is a significant industrial complex that produces a range of petroleum-based products. The facility is subject to strict environmental regulations, particularly regarding wastewater treatment and discharge. The implementation of

wastewater valorization techniques can help the refinery to reduce its dependence on external resources and improve its environmental impact.

We opted to utilize the reclaimed water in the boiler feedwater system instead of the cooling tower due to its greater complexity and challenges because it involves careful considerations and technical expertises. This approach requires rigorous treatment processes to ensure the water meets the necessary quality standards for safe and efficient boiler operation and which we'll tackle in details later on in through this work.

Chapter 2

Water Demineralization Techniques

2.1 Introduction

As discussed in Chapter , it is essential to maintain the highest water quality to ensure efficient and safe operation of boilers. Indeed, water that is high in mineral content can cause significant problems in steam generation systems, including scaling, corrosion, and a low effciency. To combat these issues, demineralization techniques are employed to reduce the concentration of minerals.

In this chapter, we will focus on the demineralization techniques that have proven to be effective in reducing the mineral content of boiler-feed water. Specifically, we will examine membranes techniques such as electrodialysis and ions exchange resins.

2.2 Membranes techniques

Membranes processes are used in a wide variety of industrial settings because they may provide benefits such as highly selective separation, continuous, automatic, and economical operation at room temperature and easy integration into already-existing production processes [8].

The following categories of membrane processes can be based primarily on the driving force used : [9]

- Pressure-driven processes, such as reverse osmosis, nanofiltration, ultrafiltration, microfiltration, or gas separation; or partial-pressure-driven processes, such as pervaporation.
- Concentration-gradient-driven processes, such as dialysis;
- Temperature-driven processes, such as membrane distillation;
- Electrical-potential-driven processes, such as electrodialysis (ED).

In this section the electrical-potential-driven processes will be tackeled. These processes are crucial for ion exchange membranes.

2.2.1 Ion exchange membranes

Ion-exchange membranes (IEM) are a novel class of polymers that can be thought of as sheet-form ion-exchange resins. The polymer matrix, the functional groups attached to the matrix, and the mobile ions absorbed on the functional groups are the three main components of ion-exchange membranes. Coions and counterions, respectively, are terms

used to describe mobile ions whose electrical charges are opposite and identical to those of the functional groups [10].

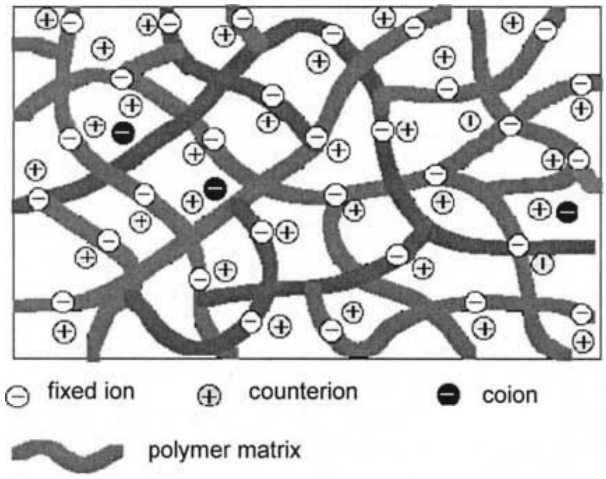

Figure 2.1: Schematic drawing illustrating the structure of a cation-exchange membrane

2.2.1.1 IEM classification

Ion exchange membranes can be categorized in a number of ways, including according to their functions, the materials that make up the membranes, their structure and microstructure, etc.

1. **Based on their function**

   - Cation and anion exchange membranes: Figure 2.1 shows a cation-exchange membrane (CEM) with fixed anions and mobile cations. The fixed negative charges are in electrical equilibrium with the mobile cations in the polymer spaces [11]. The counterions, having the same charge, are mostly excluded from the polymer matrix—a phenomenon known as "Donnan exclusion" [F.G. Donnan et al., 1932].

     If, however, the functional groupings network is charged positively and the ions that balance it are anions, the membrane only becomes permeable to anions (AEM). The reported apparent pKs of charged groups are shown in Table 2.1., the majority of which can be used as ion exchange groups in membranes;

   - Amphoteric membranes: Amphoteric ion exchange membranes have randomly arranged cation and anion exchange groups with an average separation of less than 10 Å [12]. They can be classified into four types: layer-by-layer prepared, snake cage type, polysalt, and randomly distributed cation and anion exchange group membranes; [11]

Table 2.1: Apparent pK of usable ion exchange groups for ion exchange membranes

Cation exchange groups	Apparent pK	Anions exchange groups	Apparent pK
-CF_2SO_3H	6	-$N(CH_3)_3OH$	>13
-SO_3H	0-1	-$N(CH_2OH)(CH_3)_2OH$	>13
-CF_2COOH	2	-$S(CH_3)_2OH$	>13
-COOH	4-6	-$P(CH_3)_3OH$	>13
-PO_3H_2 pK_1	2-3	NH_2	7-9
pK_2	7-8		
-Phenolic OH	9-10	-Aniline (NH_2)	5-6

- Bipolaire membranes: Bipolar membranes combine a cation exchange membrane (CEM) and an anion exchange membrane (AEM) to produce acids and bases from water. Applying an electric potential charges the CEM positively, the AEM negatively, and generates an electric field in the insulating layer; [12]
- Mosaic membranes: Mosaic membranes are composite membranes with multiple layers of different materials arranged in a mosaic pattern. They can include polymers, ceramics, metals, and carbon-based materials, serving various purposes and enhancing overall performance. [13]

2. **Based on the materials**: Based on the materials constituting the ion exchange membranes, such membranes can be classified as: [12]
   - Membranes composed of hydrocarbons or partially halogenated hydrocarbons;
   - Perfluorocarbon membranes;
   - Inorganic membranes;
   - Composite membranes of inorganic ion exchanger and organic polymer.

In recent years, naturally obtained marine polymers such as alginate and chitosan have been actively examined as materials for ion exchange membranes.

2.2.1.2 IEM characteristics and transport phenomena

The properties of ion-exchange membranes depend on the fixed ionic groups and the polymer matrix, which directly impact their fundamental characteristics.

1. **Swelling capacity**: a membrane's swelling capacity, also known as gel water content, affects its selectivity, electrical resistance, and hydraulic permeability. Mass balance, which is defined as the weight difference between the wet and dry membrane, makes it simple to determine the swelling of the membrane: [14]

$$\text{Swelling}(\%) = \left(\frac{W_{\text{wet}} - W_{\text{dry}}}{W_{\text{wet}}}\right) \times 100\% \tag{2.1}$$

   Where W_{wet} and W_{dry} are the weight of a membrane in wet and dry states.

2. **Permselectivity of Membrane**: Counterion transport ratio determines ion-exchange membrane permselectivity. Ideal permselective membranes selectively allow counterions based on Donnan exclusion, limited by membrane electroneutrality. Permselectivity is calculated using transport numbers of counterions and coions in the membrane and solutions, it's given by the next equation: [10]

$$P = \frac{T_{\text{cou}} - T_{\text{co}}}{T_{\text{co}}} = \frac{T_{\text{cou}} - T_{\text{cou}}}{1 - T_{\text{co}}} \tag{2.2}$$

   Where T_s and T_m denotes the transport number of ion in the solution and membrane, respectively; the subscripts $_{cou}$ and $_{co}$ refer to counterion and coion, respectively.

3. **Resistance of the membrane**: Ion-exchange membrane resistance affects energy consumption and cost knowing that lower resistance improves performance. Contribution to system resistance depends on electrolyte nature and concentration. However, membrane resistance is typically lower than dilute solutions due to higher ion concentration. [15]

4. **Streaming potential**: An electrical potential is created across the membrane when hydraulic pressure is applied, for example, to a negatively charged membrane.This electrical potential is lower on the upper-stream (high pressure) side of the membrane. The streaming potential, ΔE, is correlated to ζ, according to the Smoluchowski-Helmholtz equation: [10]

$$\frac{\Delta E}{\Delta P} = \frac{\epsilon \cdot \zeta}{\nu \cdot \mu} \tag{2.3}$$

Where ΔP is the pressure difference across the membrane, ϵ is the solution permittivity, and ν and μ are the viscosity and conductivity of the solution, respectively.

5. **Diffusion coefficient of the electrolyte**: In electrodialysis, an IEM separates dilute and concentrated solutions, allowing diffusion of electrolytes and non-electrolytes. Diffusion directly impacts current efficiency and product purity, making the electrolyte's diffusion coefficient crucial. The diffusion coefficient is calculated by the Fick equation and simplified: [10]

$$\Delta M = \frac{D \cdot A \cdot (C_c - C_d) \cdot t}{\delta} \tag{2.4}$$

Knowing that ΔM is the diffused amount of electrolyte, D, diffusion coefficient, A, effective membrane area, C_c and C_d, the concentrations of electrolyte in the concentrated side and the diluted, δ, thickness of the membrane, and t, diffusion period.

6. **Chemical and thermal stability**: Chemical stability and longevity of ion-exchange membranes significantly impact the economics of these processes. Membranes must with stand harsh conditions, including high temperatures, extreme pH levels,
oxidizing/reducing agents, and high concentrations of chemicals, to reduce costs and improve efficiency. [14]

7. **Mechanical strength**: Strong mechanical properties are essential to ensure the durability and longevity of the membranes. This includes the ability to resist
physical stresses, such as pressure differentials, handling during installation and maintenance, and potential deformation or damage. [15]

2.2.2 Electrodialysis

2.2.2.1 Electrodialysis principle

For a typical ED stack, as indicated in Figure 2.2 , the IEM and CEM together with the gasket are alternately arranged. Anions migrate toward the anode and pass through

anion-exchange membranes when an electrical current field is applied, but they are retained by the cation-exchange membranes due to the permselectivity of ion-exchange membranes. Similar to how anions are rejected by anion-exchange membranes while cations pass through cation-exchange membranes. In this way, a salt, acid, or base are concentrated in different compartments, and after some time of operation, the other solutions lose their ionic components. [14]

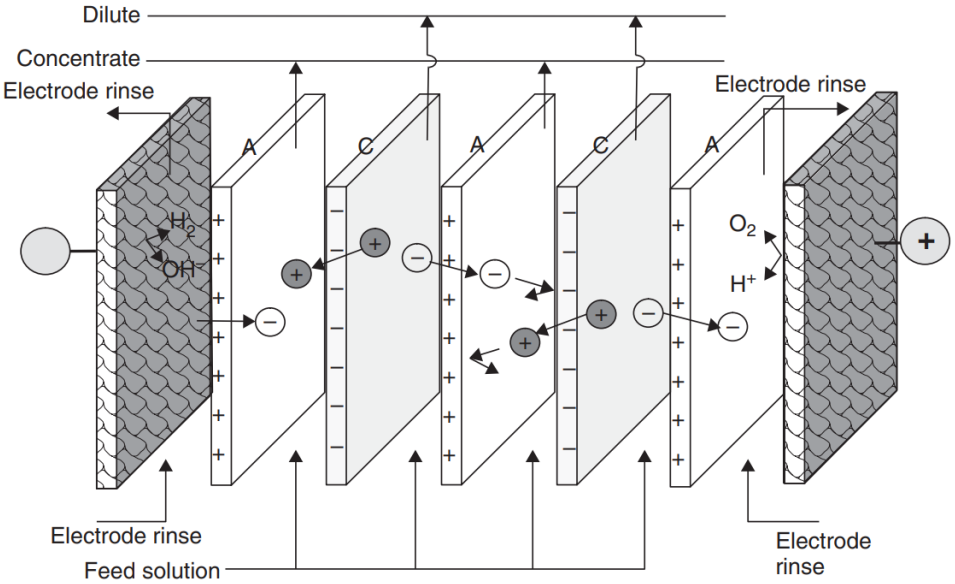

Figure 2.2: A schematic principle of ED process

2.2.2.2 Faradaic efficiency

The ratio of the actual current used to transmit a given amount of charged substances to the theoretically required current for an electrodialyzer is known as its Faradic performance. The Faradaic efficiency of monovalent ions is given by the following equation: [16]

$$R_f = \frac{(n_i - n_f)F}{I \cdot t \cdot n} \tag{2.5}$$

Where: n_i and n_f are the moles number at initial and final respectively, F, Faraday number equivalent to 96500C and I the current.

2.2.2.3 Limitation factors

- **Concentration polarization and limiting current density**: Polarization arises from diffusion boundary layers near the membrane surface due to different ion

transport numbers in the membrane and solution. The membrane carries current mostly through counter-ions, excluding co-ions, while the solution has balanced cation and anion currents. This leads to a higher rate of ion transport in the membrane, causing concentration gradients known as diffusion boundary layers near the membrane. [16] The current density value where the concentration of the ions on the membrane surface on the dilution side approaches zero, is called the limiting current density (I_{lim}) and is defined by: [16]

$$I_{\text{lim}} = \frac{C_0 \cdot D \cdot z_j \cdot F}{\delta(T_m - T_s)} \tag{2.6}$$

Where C_0 is the concentration of the salt within the solution and z_j the charge of the counter-ion.

The method that connects the applied current density (i) to the measured membrane potential (phi_m) can be used to determine the limiting current density.

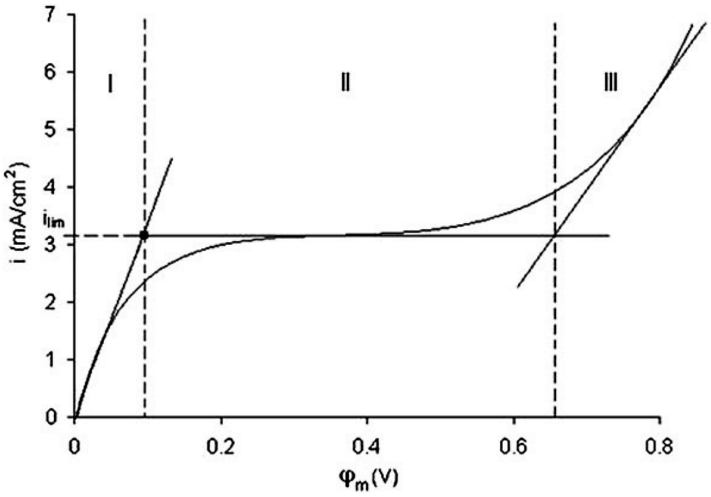

Figure 2.3: A typical current-potential curve for an ion selective membrane

On this curve as shown in Figure 2.3, there are three distinct regions that stand out: a quasi-ohmic variation of the current-voltage curves in the lower voltage range (region I), a plateau from which the value of the limiting current is derived (region II), and finally an increase in current density (region III), which can be attributed to various phenomena that occur in conjunction with concentration polarization. [17]

- **Phenomena accompanying concentration polarization**: [18]

  1. Water dissociation and exaltation effects: The attraction effect in EED is caused by the electric field generated by the H^+ and OH^- by products of water

dissociation. This field interacts with ionic species in the solution, particularly OH^- ions with positive ionic species, resulting in an increased flow of these species from the bulk of the solution to the membrane surface;

2. Gravitational convection: It occurs when a fluid with a density gradient is subjected to gravity. Concentration polarization near ion-selective membranes creates concentration gradients, resulting in temperature gradients. Gravitational convection leads to the collapse of the diffusion boundary layer and increased flow of ionic species to the membrane surface;
3. Electro-convection: Electro-convection can cause mixing between different compartments in the electrodialysis cell, reducing the selectivity of ion transport and potentially contaminating the product or waste streams;

2.2.2.4 Applications

Electrodialysis has various applications in different industries:

- **Desalination**: ED is commonly used in desalination processes to remove salt and other dissolved ions from water. It is particularly useful for brackish water desalination and can be combined with other technologies like reverse osmosis for more efficient water treatment;
- **Food and Beverage Industry**: ED is used in the food and beverage industry for various purposes. It can be utilized for desalting brine solutions, clarifying fruit juices, removing bitterness from certain products, and recovering valuable components from process streams;
- **Energy Storage**: ED has potential applications in energy storage systems, such as redox flow batteries, where it can assist in the separation and purification of electrolyte solutions.

The versatility of the technology allows it to be utilized in various sectors where selective ion separation, desalination, or purification is required.

2.3 Electrodeionization fundamentals

To boost the ED performance, and eliminate concentration polarization and high cumulative resistance, which decreases cell efficiency, ion-exchange resins (IXRs) can be inserted inside the channels. This new hybrid system was subsequently named electrodeionization (EDI) or continuous electrodeionization (CEDI). EDI is more suitable

than its source technologies for producing industrial ultra-pure water and treating some wastewater containing metal ions [19].
for several years, the complex transport mechanism and general lack of understanding as to its functional kinetics were the reason for the slow advance of this technology. To elucidate the EDI process, in 1971, Matejka described a mechanism that encompassed four simultaneous stages have been developed as the following steps [20] :

- Ion diffusion through the solution to the surface of the solid (controlling step);
- Ion exchange between the solution and the resin bed;
- Migration across the IXR bed and the ion exchange membrane IEM via the application of an electric field;
- Electrolytic regeneration of the ion exchange resin IXR.

In a CEDI device, the space within the ion-depleting compartments (and in some cases also in the ion concentration compartments) is filled with ion exchange resins. The function of the ion exchange resin is to enhance mass transfer, the resin also encourages water splitting, which is desired for this polishing ion removal technique and also reduces the resistance to electric current through the stack because conductivity (resin) is 2- 3 times more conductive than water in the ion depleted chamber (dilute chambre). [21]

2.3.1 Resin regeneration phenomenon

Ion depleted chamber, only weakly ionized material remains. As a result, polarization occurs resulting in water splitting with the subsequent release of hydronium and hydroxyl ions into the water stream (see Figure 2.4), which continuously regenerates the resin in situ without using regenerating chemicals. water splitting is greatest in the area where resin beads are in contact with each other or with the ion exchange membrane (bipolar contact). [21]

2.3.2 Limitations of EDI

Limitations in EDI performance may drive by small current efficiencies in operations with high water dissociation and from inhomogeneous flow distributions. Those issues can be resolved by identifying optimal values of the applied voltage, thus resulting in the co-existence of water dissociation and electroconvection in the over-limiting regime, which can improve the process efficiency. The latter issue can be addressed by adopting fixed wafers. [22]

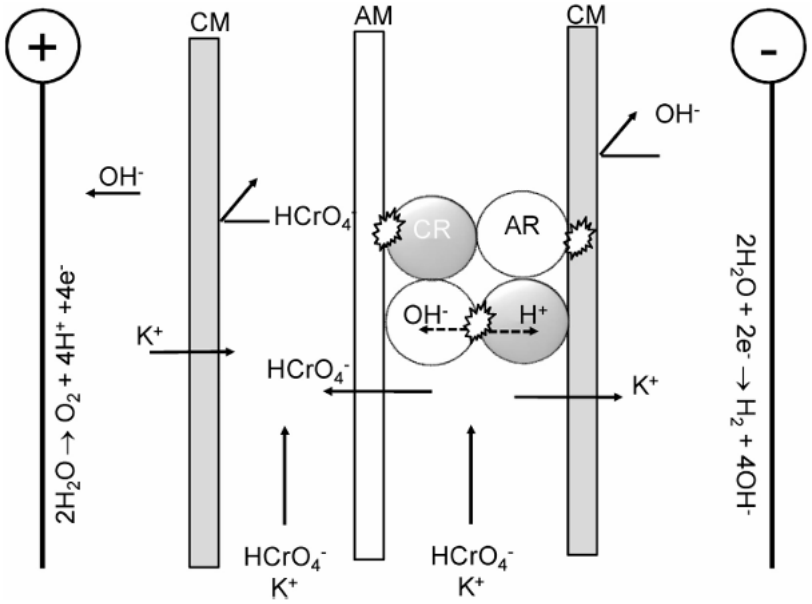

Figure 2.4: water splitting site [20]

2.4 Ion exchange resins

Ion exchange resins are insoluble polymers with covalently bonded active ionogenic groups. The fixed groups can be ionized or can accept protons to form the charged site, depending on whether they are permanently ionized, in which case they always have a formal charge. An external solution's mobile ions interact with the resin. The matrix refers to the resin's polymeric network.

2.4.1 Types and classes

Natural ion exchangers

Most naturally occurring ion exchange materials are crystalline aluminosilicates possessing cation exchange capabilities. Among these cation exchangers are zeolites such as analcime, chabazite, and natrolite. Additionally, numerous coal samples exhibit natural ion exchange properties due to the presence of carboxylic and potentially other weak-acid groups. However, a notable drawback of these materials is their propensity for significant swelling and vulnerability to alkali-induced decomposition. Therefore, it is imperative to employ stabilization techniques using solutions containing copper, chromium, or aluminum salts [23].

Inorganic ion exchangers find application in both industrial and municipal water and wastewater treatment processes. The initial applications, such as the utilization of aluminosilicates for water softening, have been further enhanced through the adoption

of synthetic resins [23].

Synthetic ion exchangers

The predominant method of producing ion exchange resins involves the copolymerization of styrene and divinylbenzene (DVB). Styrene molecules form the fundamental matrix of the resin, while DVB serves to cross-link the polymers, enabling the resin to exhibit general insolubility and durability. For water and wastewater treatment applications, ion exchange processes typically utilize resins in the size range of 20 to 50 mesh, ensuring optimal performance and efficiency. [24]

Table 2.2 demonstrates the categorization of synthetic ion exchangers into four primary classifications based on the functional group present in the resin.

Table 2.2: Classification of the major ion exchange resins

Type	Active group	Typical configuration
	Cation exchange resins	
Strong acid	Sulfonic acid	C_6H_6-SO_3H
Weak acid	Carboxylic acid	R_1-$CH_2CHCH_2(COOH)$-R_2
	Anion exchange resins	
Strong base	Quaternary ammonium	C_6H_6-$CH_2N(CH_3)_3Cl$
Weak base	Secondary amine	C_6H_6-CH_2NHR
Weak base	Teriary amine (aromatic matrix)	C_6H_6-CH_2NR_2

2.4.1.1 Synthetic cation exchangers

Cation exchangers are available with numerous fixed ionic groups exhibiting a range of different properties and acid strengths. In general, strong-acid cation exchangers substitute one ion for another depending on the resin's selectivity, and as such operate at all pH values. Weak-acid resins operate only over a limited pH range. [25]

- **Strong-acid cation exchange resins reactions :** This type of cation resins can remove, in hydrogen cycle, all major cations. The equation for removing calcium sulfate is hydrogen cycle is:

$$CaSO_4 + 2\ (R\text{-}H^+) <=> 2\ (R^-)\text{-}Ca^{2+} + H_2SO_4$$

The regeneration equation is as follow:

$$H_2SO_4 + R\text{-}Ca <=> R\text{-}H_2 + CaSO_4$$

- **Weak-acid cation exchange resins recations :** In fact, weak-acid exchangers require the presence of some alkaline species, for exemple the next reaction :

$$Ca(HCO_3)_2 + 2\ (R\text{-}H^+) <=> 2\ (R^-)\text{-}Ca^{2+} + 2(H_2CO_3)$$

2.4.1.2 Synthetic anion exchangers

Anion exchangers were almost developed exclusively as synthetic resins, organic exchangers were among the earliest ion resins exchange products. In general, strong-base anion exchangers operate at all pH values, but their capacity is less than stoichiometric, and they must be regenerated more frequently than weak-base resins, which exhibit much higher capacities and regenerate almost stoichiometrically. [25]

- **Strong-base anion exchange resins reactions :** Reaction with strong and weak acid anious such as Cl^- is as follow:

$$2(RN)OH + 2\ HCl <=> 2\ (RN)Cl + 2H_2O$$

Regenration reactions with strong bases such as NaOH is:

$$2\ (RN)Cl + 2\ NaOH <=> 2\ (RN)OH + 2NaCl$$

- **Weak-base anion exchange resins reactions :** Reaction with strong acid anions such as $SO_4{}^{2-}$ is:

$$2\ (RNH_3)OH + H_2SO_4 <=> 2\ (RNH_3)_2SO_4 + 2H_2O$$

Regeneration of the same ion using sodium carbonate is:

$$2\ (RNH_3)_2SO_4 + Na_2CO_3 + H_2O <=> 2\ (RNH_3)OH + Na_2SO_4 + CO_2$$

2.4.2 Ion exchange resins properties

1. Physical durability: physical durability becomes a concern when ion exchange resins undergo multiple recycling cycles, as they tend to fragment into smaller particles. This fragmentation can lead to headloss and reduced separation efficiency, particularly in the case of mixed beds, thereby interfering with the deionization process. [25]

2. Cross-linking: Ion exchange reactions rely on the diffusion of counter ions within the resin particles. The mesh structure of the polymer matrix significantly influences these reactions, making cross-linkage an important factor to consider when analyzing resin properties. It's worth noting that secondary cross-linkage can occur as side reactions when exchange groups are introduced into the polymer. [25]

3. Exchange capacity: Increasing the cross-linkage generally leads to an increase in exchange capacity. However, it is important to note that a higher cross-linkage also results in a slower reaction rate. Therefore, an intermediate cross-linkage of around 8% is commonly chosen as a standard for strongly acidic cation and strongly basic anion resins. [25]

4. Selectivity: The selectivity of resins for different ions generally shows the following trends [23]:

    - Fow low ions concentrations at ordinary temperature, strongly acidic ion exchange resins are more selective for ions of high valenve: $Na^{+} < Ca^{2+} < Al^{3+} < Th^{4+}$. For ions of the same ionic valence, the resins are most selective for higher atomic number: $Li^{+} < Na^{+} < Rb^{+} < Cs^{+} < Mg^{2+} < Ca^{2+} < Ba^{2+}$.
    - The selectivilty of anion exchange resins is as follows: Citrate$> I^{-} > Br^{-} > Cl^{-} >$ Acetate$> F^{-}$.
    - In high-temperature environments, nonaqueous media, or at high ion concentrations, it is observed that the exchange potentials of ions with similar valence do not increase proportionally with increasing atomic number. Instead, they tend to become very similar, reaching a plateau or even decreasing. This phenomenon can be attributed to factors such as the influence of solvent properties, ion size, charge density, and ion-ion interactions.
    - The exchange potentials of different ions can be estimated or approximated based on their activity coefficients. The activity coefficient provides a measure of the deviation from ideal behavior in a solution. In general, the higher the activity coefficient of an ion, the greater its exchange potential.

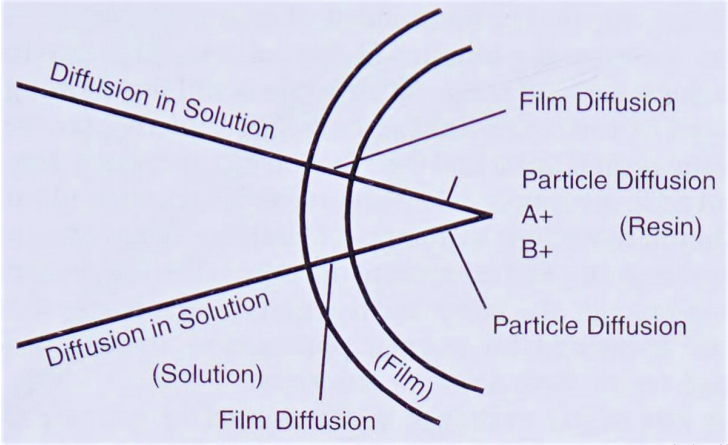

Figure 2.5: Schematic description of ion exchange process

2.4.3 Ion exchange kinetics

The ion exchange process involving a strongly acidic ion exchange resin B^+ and an electrolyte solution A^+Y^- can be described as follows: [25]

1. A^+ ions in the solution migrate across the solution-resin interface and diffuse through the macropores of the resin phase. They reach the exchange points within the resin where ion exchange reactions take place.

2. As a result of the ion exchange reaction, B^+ ions are released from the resin and escape through the micropores. They migrate across the resin-solution interface and diffuse into the solution phase.

3. At the resin-solution interface, there exists a film of solution with a concentration gradient. This region is known as the diffusion layer.

The ion exchange process can be visualized using a schematic representation, as shown in Figure 2.5.

The rate of diffusion through the resin phase is determined by the concentration of fixed charges on the resin, the effective particle-diffusion coefficient of the ions, and inversely proportional to the volume of the resin particles. [26]

Similarly, the rate of diffusion through the solution film is proportional to the concentration of the solution and the effective film diffusion coefficient of the ions. It is inversely proportional to the thickness of the diffusion layer.

These factors collectively govern the overall kinetics and efficiency of the ion exchange process.

2.4.4 Ion exchnage processes

2.4.4.1 Water sofetening

The removal of the hardness of ions Ca^{2+} and Mg^{2+} may be achieved with a strong acid cation exchanger in the Na^{+} form. Fortunately, at the low concentrations of most raw waters the resin strongly prefers the divalent cations over sodium ions, so that the exchange reaction proceeds to the right:

$$2RSO_3^- \ Na^+ + Ca^{2+} <=> (RSO_3^-)_2 \ Ca^{2+} + 2Na^+$$

2.4.4.2 Demineralization

Cation removal by a strong acid resin, with the production of protons, followed by anion removal with a strong base resin and the neutralization of the protons with the hydroxyl ion released, produces deionized water: [23]

$$RSO_3^- \ H^+ + M^+ <=> RSO_3^- \ M^+ + H^+$$

$$R_4N^+OH^- + A^- + H^+ <=> R_4N^+A^- + H_2O$$

For the production of water of high quality, the system in Figure 2.6 is employed. When the anion exchanger is a type I strong base resin the product water typically has a conductivity of 0.1 µS.cm^{-1} and a silica level of 0.01 mg.L^{-1}. With a type II strong base resin, both values will be approximately doubled. High-quality water is obtained at the expense of high consumption of mineral acid and alkali since only strong electrolyte resins are utilized. The use of a mixed bed of strong electrolyte resins also increases the capital cost of the plant and complicates its operation. [23]

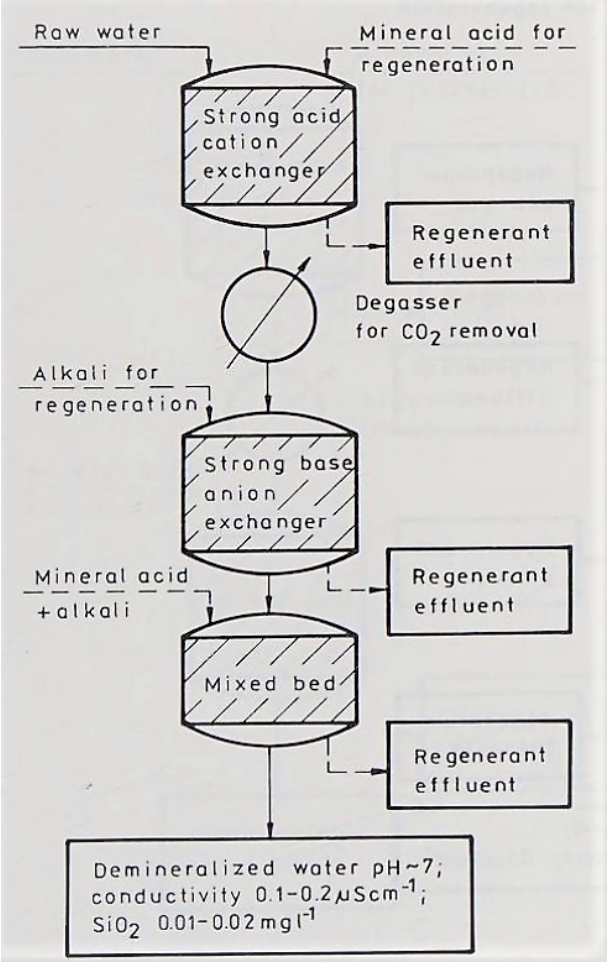

Figure 2.6: Flowsheet for producing demineralized water

2.5 Conclusion

In conclusion, following a comprehensive analysis of water demineralization techniques, ED emerges as the optimal choice. Electrodialysis demonstrates favorable attributes, including its simplicity, ease of operation, and cost-effectiveness. Additionally, the incorporation of an ion exchange resin bed synergistically complements the ED process, enhancing the overall demineralization efficiency. Through this integrated approach, efficient and economically viable removal of mineral ions is achieved, yielding high-quality demineralized water suitable for a treated wastewater demineralization.

Chapter 3

pre-treatment process

3.1 Introduction

Pre-treatment is essential when the quality of the water is poor. Pretreatment is considered at the head of an effluent treatment works, it allows purified water to be delivered to the sequential processes for more efficiency with best results.
The selection of the pre-treatment will depend on the wastewater composition and its variability. However, a step to remove solids and turbidity is essential before using activated carbon filters to remove organic [27]. The current work problem has been overcome by using activated carbon for water quality enhancement.
Activated Carbon Adsorption is utilized to remove organic contaminants. To some extent, this procedure may also be effective in the removal of inorganics. GAC is used to comply with pretreatment standards to meet the discharge limits in conjunction with others technologies such as reverse osmosis, Electrodialysis, ion exchange, and others.

3.2 Fixed-bed filtration with activated carbon

3.2.1 Adsorption phenomena

Adsorption is a surface phenomenon and a mass transfer operation in which a constituent in the liquid phase is transferred to the solid phase, although between solution/gas in the flotation process and solid/gas interfaces. The reverse of the adsorption reaction is called desorption when the adsorbed substance is released into the bulk solution. The substance that is being removed from the liquid is called adsorbate, if it binds the solid at a solid interface, the solid is called adsorbent [4].

3.2.2 Activated carbon

Activated carbons are used widely in many industrial applications like decolourizing sugar solutions, solvent recovery, volatile organic compound control, hydrogen purification, and water treatment.

Activated carbons are formed by elementary microcrystallites stacked in random orientations made by the thermal decomposition of various raw materials including hard and soft woods, rice hulls, refinery residuals, and coals followed by an activation process. There are two types of manufacturing activation, involving gas or chemical activation.

The gas activation starts first with heating in the absence of air at 400-500 $°C$ to remove volatile materials and to form small pores then steam at 1000 $°C$, carbon dioxide and flue gases can be used instead.

Chemical activation consists of using, for example, zinc chloride or phosphoric acid to produce activated carbon directly from the primer matter, although the pores seem to be larger than via steam activation. in packed beds, granular materials have particle sizes typically in the range of 0.4-2.4 mm with wide pore sizes distribution as described in the Table 3.1.

Table 3.1: Pore sizes in typical activated carbons

	Micropores	Mesopores	Macropores
Diameter (nm)	<2	2-50	>50
Pore volume ($cm^3\,g^{-1}$)	0.15-0.5	0.02-0.1	0.2-0.5
Surface area ($m^2\,g^{-1}$)	100-1000	10-100	0.5-2
Particle density 0.6-0.9 g/cm^3; Porosity 0.4-0.6)			

Carbons with liquid phase applications tend to have larger pore diameters, of the order of 3 nm or larger, and also need to be made with surfaces of the appropriate wettability. Porosities are commonly quoted based on adsorption with species such as iodine, methylene blue, benzene, carbon tetrachloride, phenol, or molasses giving rise to parameters such as the iodine number.

In general, activated carbons are hydrophobic and therefore they are used extensively for adsorbing non-specific compounds of low polarity in water treatment, although surface oxidation by heating in air at around 300 $°C$ can create some hydrophilic character to adsorb polar molecules. Once exhausted, GAC needs to be removed from the process equipment to be regenerated and reactivated in a special furnace [28].

3.2.3 Adsorption mechanism

Dissolved species and ions have a tendency to adsorb depending primarily on charge-based or physical interactions (physical adsorption). On the other hand, if the tendency to adsorb depends on the chemical identity of the adsorbate or chemical interactions between the adsorbate and the adsorbent [29]. In such cases, the adsorbate is said to be chemically adsorbed (chemical adsorption). Key elements of the two types are listed in Table 3.2.

Table 3.2: Physical and chemical adsorption properties

Parameter	Physical adsorption	Chemical adsorption
Occurrence	Most common	Rare
Process speed	Rapid, limited by mass transfer	Depends on the reaction rate with the surface
Bonding type	Nonspecific binding mechanisms such as Van der Waals forces, Vapor condensation	Specific exchange of electrons, Chemical bond at surface
Layers longer	Multiple layers	One molecular layer
Reaction type	Reversible, exothermic	Nonreversible, exothermic
Heat of adsorption	4-40 kj mol^{-1}	$<$200 kj mol^{-1}

3.2.4 Contaminants GAC can and cannot remove

Activated carbon is more effective in removing organic contaminants from water often responsible for taste, odor, and color problems, GAC filtration can also remove chlorine, pesticides, trihalomethanes (THM) primary chloroform, polychlorinated biphenyls (PCB) and polycyclic aromatic hydrocarbons. This makes GAC ideal for use both in industrial applications as well as in residential.

GAC filtration does not remove microbes, sodium, nitrates, fluoride, and hardness. heavy metals are removed only by using a very specific type of GAC filter [22]

Water and wastewater are multicomponent mixtures. Therefore, in the case of organic compounds, monitoring is commonly carried out by the use of sum collective parameters such as TOC, DOC, UV absorbance, BOD, and COD. [30]

3.2.5 Adsoption of Mixture

In wastewater treatment, mixtures of organic compounds are always encountered. Typically, there is a depression of the adsorptive capacity of individual compounds in a mixture, but the adsorption density of the adsorbent may increase with regard to one compound.

However, competing compounds are related to size, adsorptive affinities, and their

relative concentration. The techniques used to obtain multicomponent experimental isotherms can be modeled by using the single solute adsorption parameters and may also be determined including total organic carbon (TOC), dissolved organic carbon (DOC), chemical oxygen demand (COD) and dissolved organic halogen (DOH). [22]

3.2.6 Adsorption equilibrium and isotherm equations

Adsorption is an equilibrium process, when it occurs in the aqueous system the amount of material adsorbed per unit amount of adsorbent is called the adsorption density and is represented by (q). At equilibrium, for a given system composition no change can be observed in the concentration of the solute on the solid surface or in the bulk solution.

Equilibrium is usually presented using a relationship known as adsorption isotherm which expresses the adsorption density as a function of dissolved adsorbate concentration. Several models can be used for the description of the adsorption data, and Langmuir and Freundlich adsorption isotherms are the most commonly used.

1. **Langmuir adsorption isotherm (ideal localized monolayer model)** :

   The basic hypothesis Langmuir's model is based on:

   - The molecules are adsorbed on definite sites on the surface of the adsorbent,
   - Monolayer adsorption,
   - Quantity fixed depends solely by the geometry of the surface,
   - The adsorption energy is the same at all sites.

$$\frac{x}{m} = \frac{X_m b C_e}{1 + b C_e} \tag{3.1}$$

   where x/m, the amount of solute adsorbed, (x), per unit weight of adsorbent (m); C_e: equilibrium concentration of the solute; X_m = monolayer capacity; and b = a constant related to the heat of adsorption.

2. **Freundlich isotherm :** The Freundlich adsorption isotherm, originally proposed as an empirical equation, is used to describe the equilibrium for adsorbents having adsorption sites with differing site energies, such as activated carbon and many layers of adsorbate can adsorb to the surface :

$$q_A = K_A C_a^{(1/n)} \tag{3.2}$$

With K_A: Freundlich adsorption capacity parameter $(mg\,g^{-1})(l\,mg^{-1})^{\,1/n}$
1/n : Freundlich adsorption intensity parameter, unitless
The value of 1/n rarely exceeds 1, if it's close to 1 indicates high adsorption capacity at a high equilibrium concentration that rapidly diminishes at lower equilibrium concentrations covered by the isotherm [31].

3.2.7 Adsorption isotherms classification

Brunauer, Deming, and Teller classified equilibrium behavior into five types as shows Figure 3.1 :

- type I isotherm represents unimolecular adsorption to microporous adsorbents with small pores,
- type II and III isotherms represent adsorption that may extend from monolayer to multilayer and a wide range of pore size,
- type IV isotherms suggests the formation of two surface layers,
- type V isotherms represent definite saturation limits and large intermolecular attraction effects [32].

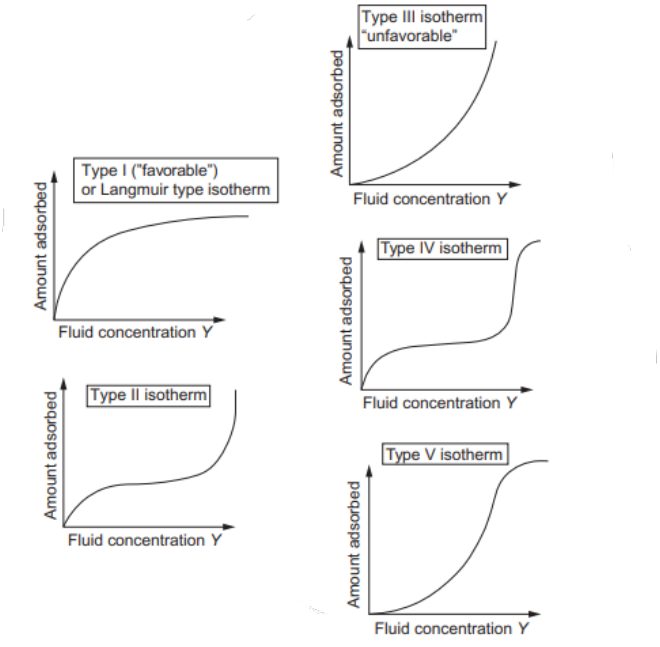

Figure 3.1: Adsorption isotherms classification

3.2.8 Factors influencing adsorption

Activated carbon adsorption depends on various factors that play a significant role in adsorption rate and magnitude. As it is difficult to predict models for all complex waste waters a brief discussion of the more important factors is presented herein.

- **Physical and chemical properties of the adsorbate :** adsorption increase with increasing molecular weight, branched-length chain, and functional groups, such as double bonds or halogens, also there is an inverse relationship between the extent of a particular solute and its solubility because high solubility reflects that the bonds with solvent are stronger than the attractive forces between the solute and the adsorbent, Activated carbon adsorbs nonpolar molecules better than polar molecules.

- **pH**: Adsorption of organic materials is higher at neutral pH. In general, adsorption is increased with decreasing pH. The extent of this effect depends on adsorbate and adsorbent charges as they can attract or repel,

- **Temperature**: the extent of adsorption increases with decreasing temperature because the adsorption reaction is exothermic, It can range from 18.3 to 32.2$°C$. However, the temperature increased the rate of diffusion of the solute through the liquid sites with also increased adsorption [27],

- **Concentration:** Concentration dependence of the rate of adsorption is used to define the rate-limiting step in the reaction, a non-linear relationship exists between removal rate and C_0 when intraparticle transport limits the kinetics of an adsorption reaction, whereas the rates of strictly adsorptive reaction and simple diffusion-controlled processes are expected to be proportional to the first power of the adsorbate's concentration [31],

- **Carbon particle size and porosity:** It is hypothesized that pore blockage is the mechanism responsible for the dependence on particle size. As GAC particle size increases, the microporous surface area behind a constricted pore also increases. The result is lower adsorption capacity per mass of adsorbent in the larger GAC particles, [33].

- **Contact time:** Time provides information on the sorption kinetics of the adsorbate for a given initial dosage of the adsorbent. At the begining the surface of the adsorbents had a high concentration of free active sites, so the adsorption speed is very fast. As the process progresse the adsorbed concentration decrease to reache the steady state.

3.2.9 Kinetics of adsorption

The adsorption kinetics can be described as four or less definable as shown in 3.3 :

1. Bulk solution transport: involves the movement of the organic material to be adsorbed through the bulk liquid to the boundary of film liquid surrounding the adsorbent surface. There is no actual film but is used to describe the resistance to mass transfer at the surface of the particle,

2. Film diffusion transport: involves the transport by diffusion of the organic material from the stagnant film to the entrance pore of the adsorbent,

3. Pore transport: involves molecular diffusion through the pore or along the surface of the adsorbent,

4. Adsorption (or sorption): involves the attachment of the adsorbate at an available adsorption site [4].

The fourth step is very rapid, it does not influence the overall kinetics. adsorption rate will be controlled by the slowest step which would be either film diffusion or pore transport.

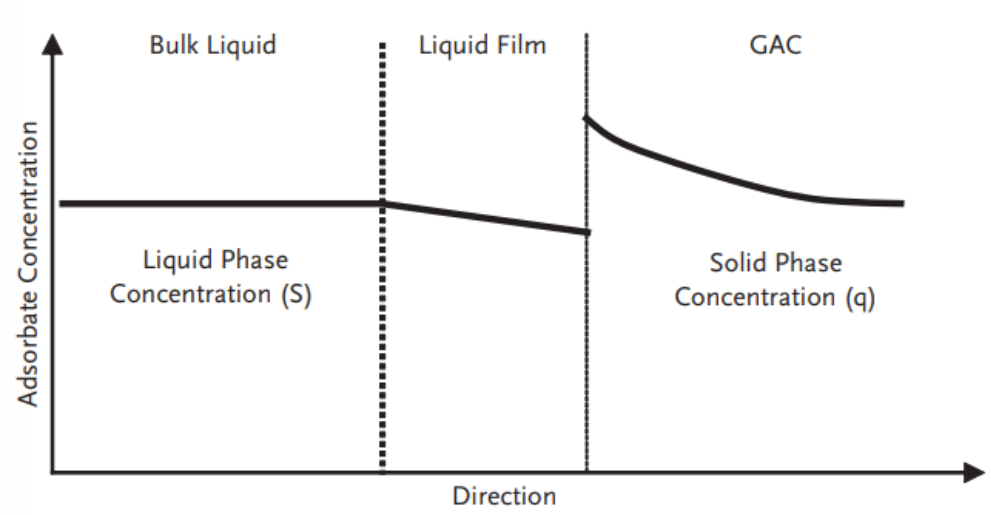

Figure 3.2: Typical Concentration profile of adsorbate in the liquid and solid phases in the case of a liquid film over carbon surface

3.2.10 Adsorption dynamics in fixed-bed adsorbers

In practical terms, fixed-bed adsorbers are more suitable for granular adsorbents than batch systems which are appropriate for the application of powdered adsorbents.

Adsorption in a fixed bed adsorber is a time and distance dependent process. equilibration proceeds successively with solution percolating, layer by layer, from the column inlet to the column outlet.

However, in natural water systems, there is a wide spectrum of organic contaminants. Competitive adsorption and displacement of weakly adsorbed compounds by strongly adsorbed ones complicate the prediction of the shape of the breakthrough curve so the mass transfer zone. therefore, previous studies must be conducted for appropriate design

3.2.10.1 The mass transfer zone and breakthrough curve

When continuous adsorption of the solute is passed through the bed a wavefront or a mass transfer zone is formed in the bed. First, the solute is adsorbed on the top layers until equilibrium with influent contaminant concentration and that portion of the bed is exhausted. In the second zone below, the dynamic adsorption is occurring where the contaminant is transferred from the liquid to the adsorbent. This zone is called the mass transfer zone, and its depth depends on hydraulic factors and the characteristics of both adsorbent and adsorbate. The depth of the MTZ is a measure of physical/ chemical resistance to mass transfer. Once formed, the mass transfer moves down through the bed until it reaches the bottom. At this time the effluent concentration begins to rise. When the breakthrough of the adsorbate begins to occur, the bed takes off-line to be generated [31].

In practical, flat breakthrough curves are generally observed that deviate from the ideal one when the external and internal mass transfer occurs very fast and the length of the MTZ would approche zero. In that case, the amount of mass adsorbed until breakthrough differs more from the saturation capacity of an adsorber, and a higher mass of the adsorbent remains unused. This study is relative when single solutes are of interest. When multiple substances are removed, competition takes place for adsorption sites on activated carbon, this leads to the separation of weakly and strongly adsorbent into their respective mass transfer zones.

- weakly adsorbing components are held in deeper parts of the column
- non-adsorbable migrate rapidly until column outlet.

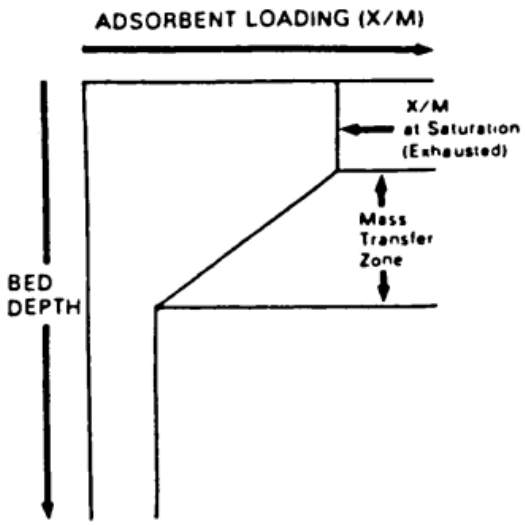

Figure 3.3: Mass transfer zone in a CAG adsorber

The plot of the effluent concentration divided by influent concentration (C/C_0) as a function of elapsed time, processed volume generates the breakthrough curve. the point at which a predetermined concentration in accordance with purity requirements is defined as the (breakthrough point). the length of the mass transfer zone is also called the critical bed depth which is the sufficient depth to prevent the effluent concentration from exceeding the desired breakthrough concentration at zero time. L_m is defined by :

$$L_m = L(1 - \frac{t_b}{t_s}) \tag{3.3}$$

With L = Total length of the bed,
t_b = Breakthrough time,
t_s = Time to saturation,

3.2.11 Major modeling approaches of fixed bed adsorbers

Before working on a large scale, it's always advisable to base the final design on detailed studies using theoretical mathematical models that simulate the application.

First, a laboratory-scale batch equilibrium study should be conducted using the selected activated carbon and the water to be treated. The common procedure is plotting data according to the Freundlich or Langmuir adsorption isotherms. The isotherm results provide information to determine the theoretical capacity, treatment feasibility,

and carbon usage rate. Once it's established, a pilot-scale continuous flow column test is conducted to determine breakthrough curves. usually, three or more columns are used in series with different contact times and depths and loaded by the amount determined previously.

The test should be continued until the breakthrough curves are fully developed for each column in the series [31]. The results of the column study are scaled up to a full-scale operation using two major designs, empty bed contact time and depth-service time proposed by Bohart-Adams.

1. **Empty bed contact time :** The major design is the empty bed contact time (EBCT). Breakthrough curves are developed by plotting the effluent concentration versus the volume processed or processing time for the column. the intersection of the desired concentration and the breakthrough curve determines the breakthrough volume.

$$EBCT = \frac{\text{bed volume } (m^3) * 7,48}{\text{flow rate}(m^3\, min^{-1})} \tag{3.4}$$

The carbon dosage is determined from :

$$\text{Usage rate } (Kg/1000\, m^3) = \frac{\text{weight of carbon in column (kg)}}{\text{volume at breakthrough } (m^3) * 1000} \tag{3.5}$$

Usefully, three or more columns are used in series to represent different bed depths and contact times. the columns are loaded with quantities of activated carbon pre-determined from the usage rate

From the data, a plot of the carbon usage rate / 1000 m^3 treated versus EBCT is constructed. The EBCT used for the design of the contactor is taken from the plot at the EBCT at the lowest carbon usage rate (see Figure 3.4) .

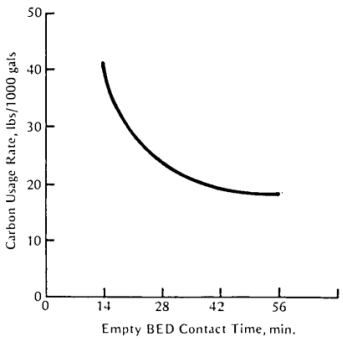

Figure 3.4: Carbon usage rate versus system residence time. Reproduced from Perrich [30], courtesy of CRC Press, Inc.

2. **Depth-service time proposed by Bohart-Adams :** Bohart-Adams model incorporates the reaction rate theory to predict the performance of a continuous flow GAC, It is extensively applied for continuous flow carbon adsorption column design, and the relationship is expressed by Equation (3.6)

$$\ln \frac{C_0}{C_e - 1} = \ln(e^{\frac{KN_0D}{v_L}} - 1) - KC_0t_b \tag{3.6}$$

With C_0 = Influent concentration of adsorbate, g l^{-1},
C_e = Breakthrough or allowable concentration of adsorbate in the effluent, g l^{-1},
K = Rate constant, $m^3\, g^{-1}\, h^{-1}$,
N_0 = Adsorptive capacity, g adsorbate /m3 activated carbon,
D = Depth of GAC bed, m,
v_L = Approaching velocity (or hydraulic loading), m h^{-1},
t_B = Breakthrough time, h.
In most cases the term $e^{\frac{KN_0D}{v_L}}$ is larger than unity so the Equation 3.6 is simplified to the Equation (3.7) :

$$tB = \frac{N_0}{C_0 v_L} D - \frac{1}{kC_0} \ln(\frac{C_0}{C_e} - 1) \tag{3.7}$$

3.3 Conclusion

This chapter discusses the adsorption phenomena in aqueous environments and major modeling approaches commonly employed in industrial plants. Due to the composition of wastewater and the requirement for high-quality treated water prior to the demineralization process, pre-treatment with granular activated carbon is considered a crucial step. Modeling equations can help predict key parameters for optimizing the overall performance of the system.

Part II

Experimental Part

Chapter 4

Materials and Methods

4.1 Wastewater characterisation measurement

Since each water treatment techniques used in this work is designed to target specific types of pollutants based on their composition and characteristics, measuring them before and after each treatment, allow us assess the effectiveness of the treatment process. The following section explains the measurement of each polluants.

4.1.1 Physical characteristics

1. **Total suspended solids (TSS) [34]**

   - Wet the filter with distilled water (DW) and dry it in the oven at 105 °C for a few minutes.
   - Take out the filter, place it in the desiccator for cooling, then weigh it on the balance until a stable weight is obtained P_1;
   - Take a 100 mL test sample, place the filter on the filtration device, and pour water volume until complete filtration;
   - Rinse the flask that contained the water to be analyzed with 10 mL of distilled water, and pass this washing water through the filter.
   - Retrieve the filter and return it to the oven at 105 °C;
   - Remove the filter from the oven and place it in the desiccator for complete cooling, then weigh the filter and record its weight P_1 .

   The TSS is calculated through the following formula:

$$\mathrm{mg}_{TSS}.\mathrm{L}^{-1} = (P_2 - P_1) \times 10 \tag{4.1}$$

2. **Turbidity**

   - Mix a sample thoroughly to disperse solids and poor it into a clean turbidity tube and place it in the turbidity meter TL-2350 (HACH).

   The turbidity is read direactly in NTU.

4.1.2 Inorganic chemical characteristics

1. **Total hardness (TH) [34]**

- In an Erlenmeyer flask or 250ml beaker, pour 100ml of water to be analyzed, add 2ml of pH 10 solution, and a pinch of eriochrome black (resulting in a dark red or violet coloration);
- While maintaining agitation, titrate with an EDTA solution (0.01M) until the color changes from dark red to blue, ensuring that the color no longer changes with the addition of an extra drop of EDTA.

The TH can be read directly from the burette graduated in mL:

$$\text{TH } (^\circ\text{f}) \ = V_{\text{EDTA}} \tag{4.2}$$

$$\text{TH } (\text{mg}_{CaCO3}.\text{L}^{-1}) \ = V_{\text{EDTA}} \times 10 \tag{4.3}$$

2. **Calcium Hardness (CaH) [34]**

- In an Erlenmeyer flask or 250ml beaker, pour 100ml of water to be analyzed;
- Add 10ml of pH 12 solution and a pinch of murexide;
- Titrate until the color changes from pink to violet.

Read the calcium hardness of the water directly from the burette:

$$\text{CaH } (^\circ\text{f}) \ = V_{\text{EDTA}} \tag{4.4}$$

$$\text{CaH } (\text{mg}_{CaCO3}.\text{L}^{-1}) \ = V_{\text{EDTA}} \times 10 \tag{4.5}$$

3. **Total Alkalinity Title (TAT) [34]**

   - Pour into a 100 ml Erlenmeyer flask the water sample to be analyzed add 1 to 2 drops of phenolphthalein;
   - Titrate with a 0.1 N sulfuric acid solution until the pink color turns colorless;
   - Add 2 drops of methyl orange and continue titrating with the same acid solution until the yellow color changes to yellow-orange and note the volum;
   - Ensure that an excess drop of acid causes the transition from yellow-orange to orange-pink color.

   The TAT is calculated according to the next formula:

$$\text{TAT } (\text{mg.L}^{-1}) = V_{\text{H2SO4}} \times 50 \tag{4.6}$$

4. **Total nitrogen (TN)**

   - Pipette 0.2 mL of the water to be analyzed and transfer it into the reaction vial;
   - Add 2.3 mL of reagent A and one tablet of reagent B. Close the reaction vial;
   - Place the vial in the reactor HT-200-S (HACH) at 120 °C for 30 minutes;
   - Remove the vial from the reactor and allow it to cool to room temperature, then invert it 3 times to mix;
   - Take 0.5 mL of the mixture and transfer it into a cuvette for total nitrogen and add 0.2 mL of reagent D and invert it 3 times to mix;
   - Set the timer to 15 minutes and thoroughly clean the outside of the cuvette;
   - When the beep sounds, insert the cuvette into the tube compartment. The recognition is automatic in the spectrophotometer UV-VIS DR-6000 (HACH) thanks to the barcode label.

   The results are displayed in (mg $_{TN}$.L^{-1}).

5. **Silica SiO_2**

   - Fill a 10 mL cuvette up and add 14 drops of Molybdate 3 reagent and agitate well;
   - Set the timer to 4 minutes and upon the beep, add the contents of one packet of Citric Acid reagent;
   - Set the timer to 1 minute and upon the beep, take the reading in the spectrophotometer recording 0.00 mg/L;
   - Fill the second cuvette with 10 mL of the sample, add 14 drops of Molybdate 3 reagent and agitate well;
   - Set the timer to 4 minutes and upon the beep add the contents of one packet of Citric Acid reagent;
   - Set the timer to 1 minute and upon the beep add the contents of one packet of Amino Acid F reagent;
   - Set the timer to 2 minutes and upon the beep and insert the prepared sample into the cuvette holder of the spectrophotometer.

   The results are indicated in ($mg_{SiO2}.L^{-1}$).

4.1.3 Organic chemical characteristics

1. **Biochemical oxygen demand (BOD) [34]**

   - For a measurement range between 0-400 $mg.L^{-1}$, the water sample taken for measurement is 164 mL;
   - Add 3 drops of Nitrification inhibitor and place a magnetic stir bar in the OxiTop IS-12 (WTW);
   - Fill the chamber with 2 pellets of NaOH and place it in the BOD bottle;
   - Close the bottle with the BOD measurement head and start the program;
   - Place the sample on the bottle rack in a refrigerator at 20 °C for 5 days.

   The final result expressed in $mg.L^{-1}$, is the displayed value read on the BOD meter multiplied by the corresponding factor for the sample which is 10.

2. **Chemical oxygen demand (COD)**

   - Turn on the COD reactor HT-200-S (HACH) and allow the temperature to stabilize at 150 °C;

- Pipette 2 mL of the water sample and introduce it into the COD tube;
- Mix the contents of the tube to obtain a homogeneous solution and place the tube in the reactor at 150 °C for two hours;
- Remove the tube from the reactor HT-200-S (HACH) and let it cool to room temperature;
- Thoroughly clean the exterior of the tube and insert the sample tube into the compartment for tubes in the spectrophotometer UV-VIS DR-6000 (HACH).

The results are indicated in ($mg_{COD}.L^{-1}$).

3. **Total oraganic carbon (TOC)**

   The TOC was analyzed through the 1030-W TOC analyzer (AURORA). The analyzer uses the proven heated persulfate Na_2SO_4 (1M) wet oxidation technique to analyze organic contamination in the aqueous samples.

4. **Phenols**

   - Measure 300 mL of DW as a blank and transfer it into the first separation funnel;
   - Measure 300 mL of wastewater and transfer it into the second separation funnel;
   - In each funnel, add 5 mL of hardness 1 Buffer and agitate well. Then add Phenol Reagent followed by Phenol Reagent 2 and agitate well to dissolve the reagents;
   - Add 30 mL of chloroform to each funnel. After closing the funnels, invert and vent them for 30 seconds, repeating this step three times;
   - Place the funnels back into the holder and allow the chloroform to separate;
   - After separation, carefully collect the chloroform phase into a 25 mL cuvette from both funnels;
   - On the spectrophotometer UV-VIS DR-6000 (HACH), input the code corresponding to the phenols measurement program and insert the blank cuvette into the cuvette holder to set the zero reading; Wipe the exterior of the second cuvette and take the reading.

   The results are indicated in ($mg_{phenols}.L^{-1}$).

4.1.4 Metal water characteristics

1. **Lead**

   - Take 100mL of the sample using a graduated cylinder and pour it into a beaker, add 1mL of pPb-1 Acid Preservative solution to the beaker using a plastic pipette, and agitate well and set the timer to 2 minutes;
   - At the beep, add 2mL of pPb-2 Fixer solution to the beaker using a plastic pipette and agitate well.
   - Gently pour the sample through the extraction column. When the flow completely stops, compress the absorbent buffer in the extractor with the piston and the dispose of the contents of the beaker and slowly remove the piston from the extractor;
   - Place a 25mL cuvette below the extractor and pour 25mL of pPb-3 Eluant solution into the extraction column using a plastic graduated cylinder;
   - Insert the piston and gently force the remaining reagent, fully compressing the absorbent buffer;
   - Add 1mL of pPb-4 Neutralizer solution to the cuvette using a plastic pipette, and agitate well, then add the pPb-5 indicator and agitate well;
   - Divide the sample by filling two 10mL cuvettes and set the timer to 2 minutes;
   - At the beep, add 3 drops of pPb-6 Decolorizer solution to one of the cuvettes, close it, and agitate well. Mark the cuvette as the blank.
   - Insert the blank into the cuvette holder in the spectrophotometer UV-VIS DR-6000 (HACH), press zero. The display shows: 0.00 mg/L.
   - Insert the second cuvette containing the sample into the cuvette holderpress measure.

   The results are indicated in $\mathrm{mg}_{Pb2+}.\mathrm{L}^{-1}$.

2. **Cyanide**

   - Fill a cuvette with 10 ml of sample, add the contents of one packet of CyaniVer 3 cyanide reagent powder, close the sample cell and shake the sample cell for 30 seconds. Allow the sample cell to rest for an additional 30 seconds;
   - Add the contents of one packet of CyaniVer 4 cyanide reagent powder and close the sample cell. Shake the sample cell for 10 seconds. Proceed immediately to the next step. Delaying for more than 30 seconds will yield weak results;

- Add the contents of one packet of CyaniVer 5 cyanide reagent powder and close the sample cell. Vigorously shake the sample cell. If the sample contains cyanide, a pink color will appear;
- Start the timer on the device. A 30-minute reaction time begins. The solution will turn pink and then blue;
- Prepare the blank: at the end of the timer, fill a second cell with 10 ml of sample. Clean the sample cell as a blank. Insert the blank into the cell holder in the spectrophotometer UV-VIS DR-6000 (HACH) and press zero;
- Insert the prepared sample into the cell holder;
- Insert the second cuvette containing the sample into the cuvette holderpress and measure.

The results are indicated in $mg_{CN-}.L^{-1}$.

3. **Chloride [34]**

   - In a 250ml beaker, add 100ml of water to be analyzed;
   - Add 2 to 3 drops of potassium chromate solution (10%);
   - Slowly add the silver nitrate solution (0.1N) while stirring with a magnetic stirrer until a reddish precipitate appears; this color should persist.

   The chloride content expressed in $mg.L^{-1}$ is given by the following formula:

$$[Cl^-] = \frac{V_{AgNO3} \times N \times 35.5 \times 100}{V} \tag{4.7}$$

4. **Sodium, zinc and Iron:** The flame atomic absorption spectroscopy (FAAS) was used to analyze the presence of Na^+, Zn^{2+} and Fe $^{2+}$ through 240-FSAA (AGILENT).

4.2 Pre-tretment on activated carbon

Activated carbon is used to remove organic matter, as discussed in section 3.2.4, including the targeted pollutant in this work, total organic carbon. Additionally, due to high total suspended solids, the wastewater is pre-filtered using a paper filter to reduce solid particles. These pretreatment steps improve the effectiveness of subsequent demineralization processes.

4.2.1 Rinsing the activated carbon used

The used commercial granulated activated carbon (GAC) was rinsed multiple times with distilled water to eliminate impurities. Subsequently, 100 g of the activated carbon was placed in a beaker with 700 ml of distilled water and heated on a hot plate at 200 °C for 30 minutes. Then, the charcoal was dried in an oven at 85 °C for 4 hours as shown in Figure 4.1 .

Figure 4.1: Commercial granulated activated carbon

4.2.2 Modelling of adsorption kinetics in batch mode

4.2.2.1 Determination of operating parameters

This section of the study focused on examining the effects of contact time and mass on adsorption using activated carbon. The goal was to determine the optimal parameters for establishing Langmuir and Freundlich isotherms.

1. **Contact time study effect**: The aim of this study is to monitor changes in pollutant concentration as a function of time. After which we note the time at

which the concentration remains constant, i.e. the saturation time. The operating parameters are summarized in Table 4.1.

Withdraw small aliquots of the mixture at 5-minutes interval and analyze the adsorbate concentration using a TOC analyzer. Plot the data against contact time to obtain a kinetic curve using the followed equation:

$$R(\%) = \left(\frac{C_0 - C_e}{C_0}\right) \times 100 \tag{4.8}$$

Table 4.1: Contact time study operating parameters

Operating parameters	GAC dose	WW volume	Duration	Stiring speed
Values	20 g.L^{-1}	0.2 L	2.5 h	200 RPM

2. **Effect of adsorbent dose**: The aim is to determine optimum GAC concentration, during which adsorption efficiency were different.The operating parameters are shown in Table 4.2. To measure the adsorption yield, apply the equation (4.8) and plot the adsorption efficiency as a function of the activated carbon dose.

Table 4.2: Adsorbent dose study operating parameters

Operating parameters	GAC mass	WW volume	Duration	Stiring speed
Values	5 to 35 g.L^{-1}	0.2 L	4 h	200 RPM

4.2.2.2 Development of adsorption isotherms

The experimental set-up is as follows: set up 4 duplicate beakers, each labeled accordingly in which 0.2L of the wastewater is poured, add: 2.5, 10.5, 14.5 and 18.5 g.L^{-1} of GAC dose to the beakers and stir the contents of each beaker at a constant speed 200 RPM. The minimum time allowed for the samples to equilibrate is 2h. At the end of four hours duration, filter the samples to remove any remaining activated carbon and measure the concentration of the TOC in each sample [4]. The experimental set-up is presented in Figure 4.2.

Figure 4.2: Experimental setp-up of the adsorption isotherms

4.2.3 GAC bed design through dynamic adsorption

The scale-up approach in GAC bed design allows the prediction of performance and optimization of design parameters. In this section, the focus was on dynamic adsorption where experiments were conducted using a laboratory set-up as described below.

4.2.3.1 Description of the experimental apparatus

The feed tank containing wastewater is connected to the peristaltic pump PR-2003 (SELECTA), which is related to the adsorption column, ensuring a secure and tight connection as shown in Figure 4.3. Place 15 g of GAC into the adsorption column ensuring it is evenly distributed and then rinse twice with distilled water.

Set the flow rate of the peristaltic pump 30 ml.min^{-1}, start the pump and begin recording time as soon as the flow is initiated and continuously monitor and record the volume of wastewater passing through the column, measuring the breakthrough volume along with the corresponding effluent concentration measured as mg$_{TOC}$.L^{-1} [6]. Ultimately, draw the breakthrough curve from the data collected.

4.2.3.2 Design methodology using Thomas equation

The Thomas model is widely utilized for designing continuous flow carbon adsorption columns by integrating the principles of reaction rate theory. This relationship is expressed by equation (4.10):

$$\frac{C_e}{C_0} = \frac{1}{1 + e^{k_1/(Q(q_0 M - C_0 V_b))}} \tag{4.9}$$

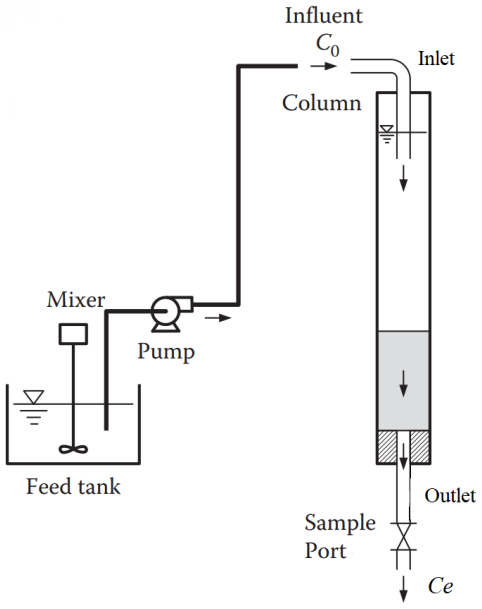

Figure 4.3: Experimental apparatus to develop design data from GAC column

where:

k_1 = rate constant, L/(mg adsorbate)·h or m^3 /(g adsorbate)·h

q_0 = maximum solid-phase concentration of adsorbate adsorbed by adsorbent, mg $_{TOC}$· g_{GAC} $^{-1}$.

Q = flow rate, $m^3.h^{-1}$.

M = mass of adsorbent activated carbon, Kg.

V_B = breakthrough volume per cycle, m^3.

C_0= influent concentration of adsorbate, $mg.L^{-1}$.

C_e = breakthrough or allowable concentration of adsorbate in the effluent, $mg.L^{-1}$.

The approach to design is as follows:

1. Plot the curve relating C_e and V_B.
2. Determine the values of k_1, and q_0 from the fit curve.
3. Determine the mass of GAC, M_{design} required in the full-scale column and the empty bed volume (EBV) carbon requirement per unit wastewater, $M_{design}/V_{B,design}$
4. Calculate the volume and dimensions of the GAC bed:

$$EBV_{\text{design}} = \frac{M_{\text{design}}}{\rho_{\text{GAC}}} \tag{4.10}$$

Cross-sectional area of the GAC bed at $v_L = 5\text{m.h}^{-1}$:

$$A_{\text{design}} = \frac{Q_{\text{design}}}{v_L} \tag{4.11}$$

Diameter of the GAC bed:

$$d_{\text{design}} = \sqrt{\frac{4A_{\text{design}}}{\pi}} \tag{4.12}$$

Depth of the GAC bed:

$$D_{\text{design}} = \frac{EBV_{\text{design}}}{A_{\text{design}}} \tag{4.13}$$

5. Calculate the liquid flow rate in terms of EBV per unit time (q_b):

$$q_{b,\text{design}} = \frac{Q_{\text{design}}}{EBV_{\text{design}}} \tag{4.14}$$

6. Calculate the service time:

$$t_{B,\text{design}} = \frac{V_{B,\text{design}}}{Q_{\text{design}}} \tag{4.15}$$

4.2.4 Pretreatment on activated carbon test

To carry out the feasibility study of the pre-treatment and to confirm the validity of the proposed process, 20 L of the real refinery's effluent was treated in the labotary.

This volume was preatreted as follow in batch mode:

- Divide the volume of wastewater into 0.7 L portions for individual testing where a 20 mg.L^{-1} dose of adsorbent was added (according to section 4.2.2.1 results)
- Stir at a speed of 200 RPM for 3 hours.
- Filter the treated wastewater and measure the TOC content.

4.3 Deminiralization using electrodialysis

4.3.1 Description of Laboratory pilote

The electrodialysis system used is of the P1 type with two compartments, consisting of 19 anionic membranes and 20 cationic membranes, each with an usable surface area of 0,69 m^2. At both ends, electrodes are located. The module is traversed by three hydraulic circuits of 2L capacity (dilute circuit, concentration circuit, and electrode rinsing circuit). The piping is made of plastic, which offers the advantage of being an electrical insulator. Elements description that constitutes the electrodialysis is summarized in Table 4.3.

Table 4.3: Electrodialysis Pilot

	Description
Pilot-scale electrodialysis	Aqualyzer from CORNING company
Membranes types	AMV type
	CMV type
Electrodes	graphite
Pompes	SieBec 38 600 Fontaine 1340 l/h
The power supply device	MCP Lab electronics M10-TP3003L

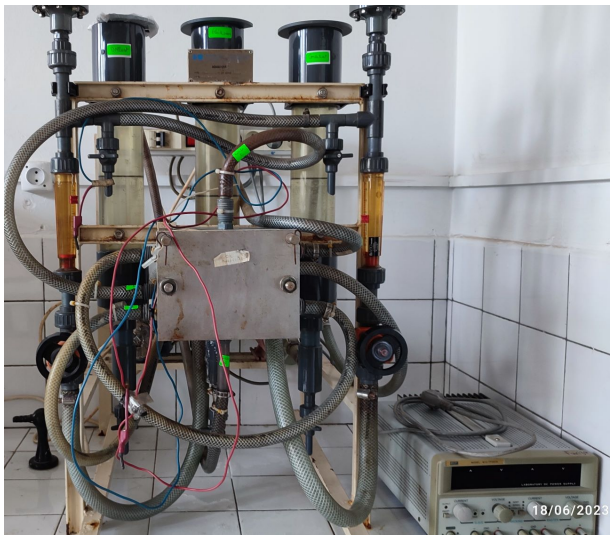

Figure 4.4: Electrodialysis module P1.

4.3.2 The cleaning and rinsing procedure

Before filling the electrodialysis system with the effluent to be treated, it is recommended to perform several washes before starting the process. Also, for all configuration, the electrodialysis cell was rinsed, between treatments, with distilled water

4.3.3 Determination of limiting current

It is important not to exceed the critical current to prevent irreversible damage to the stack. This critical current value is dependent on the solution and its concentration.
the experiment are conducted at room temperature, the hydraulic circuits are filled as follows :

- Concentration circuit: 700ml of NaCl solution 1 g L^{-1};
- Dilute circuit: 700ml of refinery treated effluent with initial conductivity of 2,01 μS cm^{-1};
- Electrode rinsing circuit: 1L of Na_2SO_4 solution 10 g L^{-1} to avoid the generation of chlorine or hypochlorite.

The procedure involves gradually increasing the current between the stack and recording the corresponding voltage displayed on the digital screen. The plot of the I-V curve exhibits a plateau, which corresponds to the limiting current.

4.3.4 Optimization of operating parameters using response surface method for the design of experiments (DOA)

To ascertain the optimal operating conditions for the electrodialysis process. It was employed a comprehensive approach consisting of two stages.

In the first stage, preliminary studies were conducted to identify the key factors significantly impacting the process. These initial experiments allowed us to narrow down the variables and focus on those with the greatest influence on the performance of the electrodialysis system and their relative zones.

Building upon the results of the preliminary studies, it was proceeded to the second stage, where Box-Behnken design was employed. This advanced experimental design allowed to systematically investigate the interaction of factors and optimize the safe operating zone of the experimental parameters.

The combination of the preliminary studies and the Box-Behnken design provided a robust experimental plan, ensuring a comprehensive analysis of the key factors and their optimal levels for achieving superior performance in the electrodialysis process.

Mathematical modeling

Considering all the linear terms, square terms and linear by linear interaction items, the quadratic response model can be described as

$$\hat{y}_i = b_0 + \sum_{j=1}^{k} b_j X_{jj} + + \sum_{j=1}^{k-1} \sum_{m=2}^{k} b_{jm} X_{ij} X_{im} + \sum_{j=1}^{k} b_{jj} X_{ij}^2 \tag{4.16}$$

With i : experience number, range from 1 to N,
X_{ij} : factor j level in the experience i,
$\hat{y}_i$: respons result calculated in the experience i,
b_0, b_j, b_{jm}, b_{jj} : model coefficients.

However, there is always a residue between the measured value (y_i) and the value calculated from the model ($\hat{y}_i$) defined by : $\hat{y}_i = y_i + r_i$.

Quality assessment of the fit

The estimation of coefficient values is based on the least squares method to verify if the model accurately summarizes the results of the experiments using four statistical models.

- Determination whether the association between the response and the term is statistically significant. it return to compare the p-value for the term to the significant level ($\alpha = 0,05$) of null hypothesis.

  if p-value $\leq$ 0,05 : there is a statistically significant association between the response variable and the term else the model is refit without the term.

- The coefficient of determination for multilinear regression, R^2;
- The coefficient of determination adjusted, R_A^2 adjusted
- Graphical analysis of residuals: a means of verifying if the residuals r_i are normally distributed around zero.

Model validation

Model validation i.e., ensuring that its predictive quality is good across the entire study domain before starting exploitation. Two validation methods are employed:

- Analysis of lack of fit : The model is validated if the variance due to lack of fit is not significant, meaning that the F_Δ ratio is lower than the critical value of Fisher.

$$F_\Delta = \frac{SS_\Delta / v_\Delta}{SS_E / v_E} \tag{4.17}$$

- Validation by test points involves comparing the measured values at points within the study domain to those calculated from the model. The model is validated if the t_exp ratios are **lower than the critical value of Student** (at 95% confidence level for the given degrees of freedom).

$$t_{exp} = \frac{y_i - \hat{y}_i}{\sqrt{\sigma^2_{\Delta y}}} \tag{4.18}$$

Model exploitation

This model can be exploited mathematically and graphically to determine the optimum using differents tools for interpretation :

- **Optimal path method :**This method involves searching for the optimum levels of the variables within the constraint for every hypersphere with a radius R (varying from 0 to the limit of the domain). The constraint is defined as the sum $\sum_{j=1}^{k} X_j^2 = R^2$. The set of points obtained constitutes the optimal path,

- **Graphical representation of response curves and response surfaces:** Graphically, this is done by plotting 2D curves that connect the points where the calculated response has the same value (called isoresponse curves). Each time, two variables are chosen while fixing the others. By adding a third dimension to the graph of isoresponse curves to indicate the values of the response, a surface of response is obtained based on the levels of the two chosen factors,

- **Study of desirability function for multiple responses :** This method aims to search for a compromise zone among various specifications during multi-response optimization. The objectives for each response are translated into elementary desirability functions that express the percentage of satisfaction based on the response value. The desirability function, denoted as d_i, is minimal (null) when it is outside the specification limits and maximal when it meets all the required conditions. The coordinates of an acceptable compromise are determined by combining the di values using the global desirability function, denoted as D defined

by Equation (4.19) [35].

$$D = (d_1 d_2 \dots d_n)^{1/n} \tag{4.19}$$

4.3.5 Application of Box-Behnken design

The experimental matrix of Box-Behnken is a three-factor design consisting of 12 experiments, with three experiments at the center of the study domain. By carefully selecting the three levels of each variable within the design, valuable data were gathered on the interrelationships between the factors and their impact on the electrodialysis process.

The dilute, concentrate, and electrode solutions were circulated with a fixed flow rate of 25 L h^{-1} and constant current until the voltage reached maximal value (32 V) which corresponded to the operating time.

The electrical conductivity that came from the dilute was measured with a conductivity meter (HANNA). NaOH was employed for pH adjustments.

The data are analyzed using the software Stat Ease-360.

4.4 Refining treatment using resins

The ion exchange column used consists of a layers bed containing 10g as mass for both types of resin. The length of the bed is 50 cm, and the diameter of the column is 1 cm as shown in Figure 4.5. Before introducing the resins into the bed, they are regenerated. The strong anion exchange resin is regenerated using a concentrated sodium hydroxide (NaOH) solution at 3%, while the weak cation exchange resin is regenerated using a hydrochloric acid (HCl) solution at 3%. Subsequently, the resins are thoroughly rinsed with distilled water until complete removal of the regenerate from the interstitial liquid.

Once the bed is fully in the H^+ and Cl^- form, the column is ready to be supplied with the treated water from the electrodialysis process (V=500ml). Main characteristics of exchange resins are summarized in the table Table 4.4. and Table 4.5. as below:

Table 4.4: Properties of the resin Amberlite IRA -420 [**?**]

Property	Value
Type	Anion exchange resin
Functionality	$N^+(CH_3)_3$
Standard ionic form	Cl^-
Bulk density	670 g L^{-1}
Total capacity	3.8 meq g^{-1}
Regenerant concentration in water %	2-4
pH Range	0-14

Table 4.5: Properties of the resin Amberlite IRC -50 [**?**]

Property	Value
Type	Cation exchange resin
Functionality	Carboxyl-COOH
Standard ionic form	H^+
Bulk density	700 g L^{-1}
Total capacity	$\geq$ 10 meq g^{-1}
Regenerant concentration in water %	2-3
pH Range	5-14

Figure 4.5: Resin bed

4.4.1 Methode of design for cation and anion demineralizer

The volume of bed per cycle is calculated using the equation 4.20. In practical applications, due to factors such as short circuiting and operational and design constraints, the actual volume of the bed is typically 1.2 to 1.5 times larger than the theoretical volume. In this specific example, a factor of 1.5 is used to account for these considerations.

$$V_R = \frac{M_{cation,anion}}{EC} \tag{4.20}$$

With M = Total quantity of cations or anion exchanged per cycle
EC = Exchange capacity of the resin

In practice, because of short circuits and other operational and design limitations, the required volume of the bed is usually 1.2–1.5 times the theoretical volume [6].
Dimensions of each Column where diameter = 1 m,

$$\text{surface area} = \pi R^2 \tag{4.21}$$

$$\text{resin depth} = V_R/S. \tag{4.22}$$

4.5 Demineralization trials using Electrodeionization

The purpose of this study was to test the feasibility of create an electrodeionizer from unemployed electrodialysis EUR 2 D-5 P. Implementing ion-exchange resins further improves the purification performance of a conventionnel electrodialysis with the same characteristics

4.5.1 EDI Setup and configuration

The laboratory-scale EDI unit consists of an EDI stack, a concentration tank, a diluent tank, an electrolyte tank, three centrifugal pumps, and a DC power supply (see figure 4.6). The EDI stack is divided into three compartments: cathode and anode, concentrate , and diluent . Two anion exchange membranes (AEM) and three cation exchange membranes (CEM) separate the compartments. The diluent compartment is filled with a 42g of equal mixed bed of cationic and anionic ion exchange resins. The main characteristics of the EDI cell are summarized in the below Table 4.6..

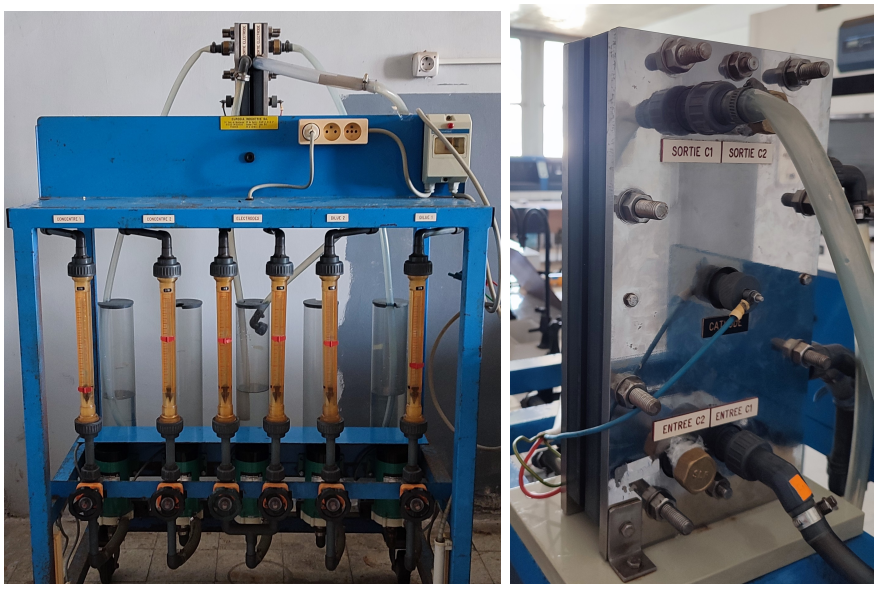

Figure 4.6: Electrodialysis stack used

Table 4.6: Technical description of the electrodialysis stack

Membranes Neosepta- Tokuyama Corp	
Cation	MEC - CMX
Anion	MEA - AMX
Effective surface par membrane	2 dm
Separator frame	
Gasket	EPDM
Spacer and slot	PE + PP
Electrodes	
Anode	Platinized titanium
Cathode	Stainless Steel 316
Electrode block and grid	PVC
Clamping plate	Stainless Steel

Material and Solution preparation

Before placing the membranes in the EDI stack, the ion exchange membranes are immersed in a salt solution for preservation. They are then rinsed with distilled water to ensure cleanliness and removal of any residual substances.

The resins used in the purification process are prepared following the same procedure described in section 4.4.

The influent is treated by passing it through a suitable quantity of activated carbon continuously. The activated carbon helps in the removal of impurities from the influent. Table 4.7 indicates initial parameters in hydraulic circuit.

Table 4.7: Feeding solution parameters for EDI treatment

Hydraulic circuits	Feeding solution
Diluent circuit	Treated effluent $\sigma_0 = 828\,\mu S\,cm^{-1}$
Concentrate circuit	Solution of NaCL $\sigma_0 = 541\,\mu S\,cm^{-1}$
Electrodat circuit	$10\,g\,L^{-1}$ of Sodium sulfate Na_2SO_4

4.5.2 Mode determination of limiting current - electrodeionisation

The determination of limiting current densities is achieved experimentally using the method described in section 4.3.3

To assess the operation of the system, the solutions introduced during the determination of the limiting current continued to circulate in the compartments of the EDI with an optimized current of 0.06 A while measuring the conductivity of the diluent and concentrate compartments at regular time intervals.

Chapter 5

Results and Discussion

5.1 Wastewater caracterisation

The wastewater obtained from Algiers's Refinery was thoroughly characterized and shown in figure 5.19. The summarized results are presented in Table 5.1 and compared to the Algerian Effluent Discharge Parameters. [36]

The analysis revealed a TSS of 79.0 $mg.L^{-1}$ and a turbidity of 33.7 $mg.L^{-1}$ at 22.9 °C. The presence of TOC and TN indicates the availability of nutrients that can stimulate the growth of microorganisms, resulting in a quantified BOD_5 level of 150 $mg.L^{-1}$. Given the nature of the refinery, which is involved in processing hydrocarbons, the elevated levels of TOC as 91.08 $mg.L^{-1}$ and COD as 111 $mg.L^{-1}$ in the wastewater are anticipated. The measured TH value of 91.2 $mg_{CaCO3}.L^{-1}$ indicates a moderate hardness classification [37]. The wastewater exhibits a pH of 7.5 representing a neutral solution along with high levels of salinity water conductivity 2.12 $mS.cm^{-1}$ [37]. The mineral characteristics exhibit trace amounts of zinc and lead, a minor presence of iron and cyanide, and notable levels of chloride and sodium, which can be attributed to the use sodium compounds in industrial processes, such hydrocracking and catalyst regeneration.

On the other hand, the calculated COD/BOD_5 ratio of 0.74, which is less than 3, indicates that the effluent is highly biodegradable. Based on these findings, it is advisable to employ granular activated carbon (GAC) adsorption as an initial step for organic matter removal to prevent pipe blockages, followed by a subsequent demineralization process.

Table 5.1: Comparison of the physico-chemical characteristics of the refinery discharge water with Algerian standards

Parameter	**Unit**	**Value**	**Limit value described by Algerian standards**
TSS	$mg.L^{-1}$	79.0	600
Turbidity	NTU	33.7	/
Temperature	C	22.9	> 30
Conductivity	$mS.cm^{-1}$	2.12	/
pH	/	7.5	5.5-8.5
TH	$mg_{CaCO3}.L^{-1}$	91.2	/
CaH	$mg_{CaCO3}.L^{-1}$	60.3	/
TN	$mg.L^{-1}$	20.86	150
TOC	$mg.L^{-1}$	91.08	/
BOD_5	$mg.L^{-1}$	150	500
Phenols	$mg.L^{-1}$	0.9	1
COD	$mg.L^{-1}$	111.0	1000
Lead	$mg.L^{-1}$	0.00	0.5
Cyanide	$mg.L^{-1}$	***0.29***	0.1
Chloride	$mg.L^{-1}$	***21.6***	3
Sodium	$mg.L^{-1}$	416.0	/
Zinc	$mg.L^{-1}$	0.00	2
Iron	$mg.L^{-1}$	0.85	1

5.2 Pre-treatement on GAC

Before applying demineralization techniques, it is necessary to pretreat the refinery wastewater rich in organic matter as indicated in section 5.1.

5.2.1 Modelling of isotherms kinetics in batch mode

5.2.1.1 Time contact study effect

The Figure 5.1 illustrates the relationship between time (t) and the adsorption efficiency (R) of the TOC on granulated activated carbon (GAC). The curve exhibits an initial steep increase in adsorption efficiency, followed by a gradual approach towards a maximum level. After reaching the peak, the efficiency remains relatively stable. The maximum yield of 97.75% is achieved at a time of 45 minutes. This indicates that the majority of the TOC is rapidly adsorbed onto the GAC within the first minutes, with diminishing gains as time progresses.

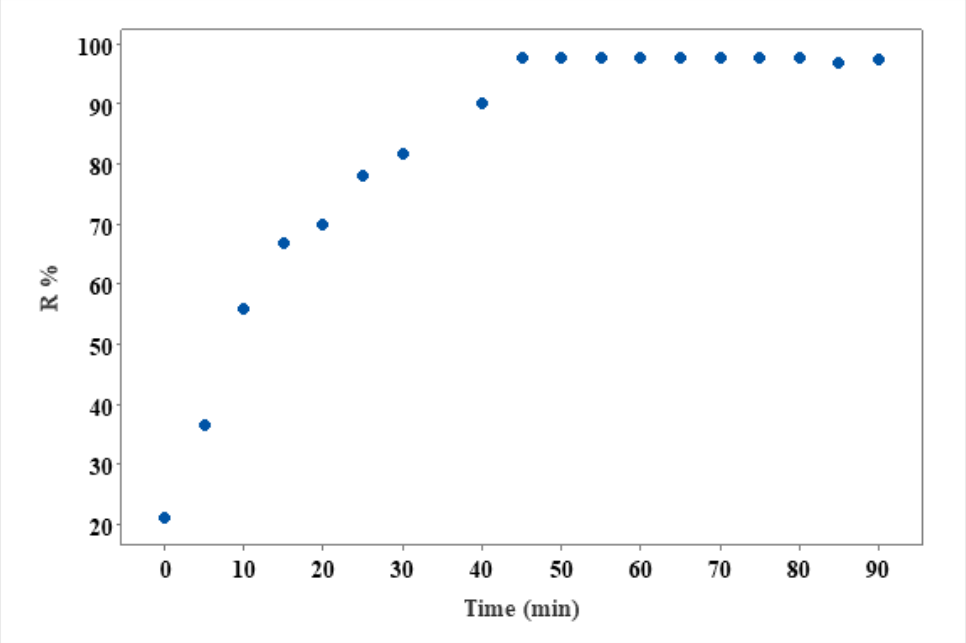

Figure 5.1: Adsorption kinetics of TOC on activated carbon
GAC dose= 20 g.L^{-1}, time= 1.5 h, stirring speed= 200 RPM.

The shape of the curve can be attributed to several phenomena. Initially, the GAC surface area is predominantly vacant, leading to a higher adsorption rate and thus a steep rise in efficiency. As time passes, the available surface sites on the GAC gradually become occupied by TOC molecules, resulting in a slower adsorption rate and a plateau in the

efficiency curve [38]. A comparative analysis was conducted, referencing the study by Mohammad-Pajooh, E & al. (2018) [39], which explored similar adsorption processes of TOC on GAC in refinery wastewater. The findings from this study aligned with the observed trend, validating the effectiveness of the adsorption process.

5.2.1.2 Effect of adsorbent dose

Based on the Figure 5.2, it is evident that increasing the adsorbant dose leads to improved adsorption efficiency. A concentration of 5 mg.L^{-1} exhibited a remarkable adsorption efficiency of 77.9%, highlighting the high capacity of the activated carbon for TOC removal. Subsequent increases in GAC dose to 10 g.L^{-1}, 15 g.L^{-1} and 20 g.L^{-1} yielded higher efficiencies of 90.9%, 94.7% and 97.6%, respectively, indicating a plateau in adsorption efficiency from 20 g to 30 g.L^{-1}.

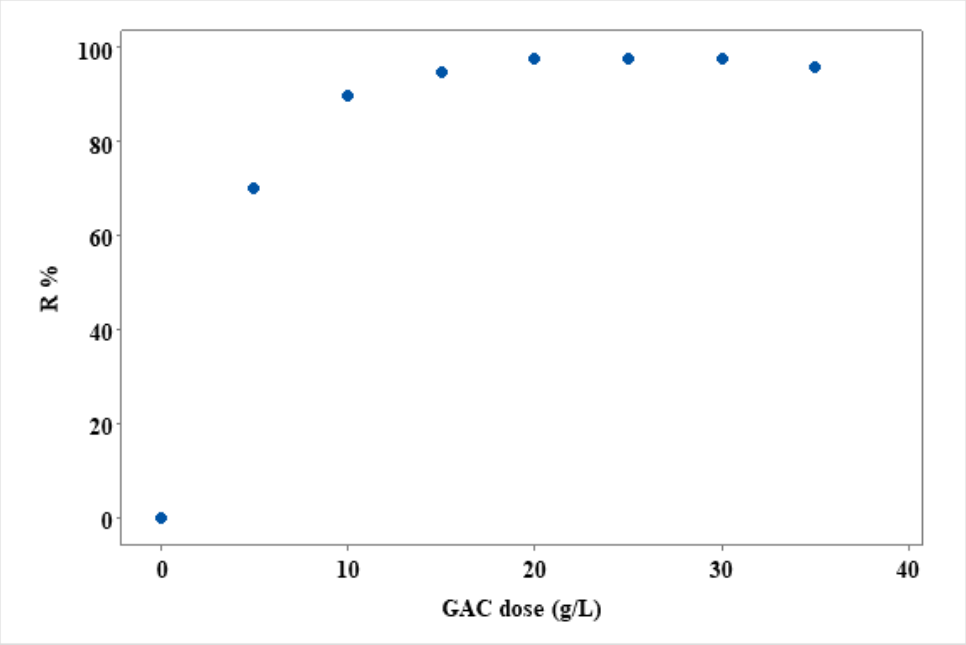

Figure 5.2: Plot of effect of adsorbent dose
GAC dose= 5-35 g.L^{-1}, time= 4 h, stirring speed= 200 RPM.

The adsorption efficiency of GAC initially improves significantly with increasing the GAC dose due to the additional surface area available for TOC adsorption. However, beyond a certain point, adding more actiavted carbon does not significantly enhance adsorption efficiency. This is because the available adsorption sites become saturated, reaching the maximum utilization of GAC surface area. Consequently, further increases in GAC mass have reached a plateau [38].

The study by W. Xing & al. (2008) [40] also investigated the adsorption behavior of DOC on GAC from industrial wastewater and reported a similar curve with increasing adsorption efficiency at lower GAC masses, followed by a plateau or stabilization at higher GAC dose which were 98.1%.

Based on the findings discussed in the sections 5.2.1.1 and 5.2.1.2, it has been determined that the optimal GAC dose for establishing the isotherms ranges from 2.5 to 18.5 g.L^{-1}. Additionally, a treatment duration of 2 hours has been identified as sufficient.

5.2.1.3 The isotherms of TOC adsorption

Figures 5.3 and 5.4 show the graphs obtained using *lsqcurvefit* regression for the plot of the Langmuir and Freundlich isotherms. With the aid of these isotherms, equilibrium values for the TOC adsorption were established. The equilibrium values and formulae found in the Langmuir and Freundlich isotherm graphs were used for obtaining the TOC adsorption isotherm constants and isotherm regression coefficients in Table 5.2.

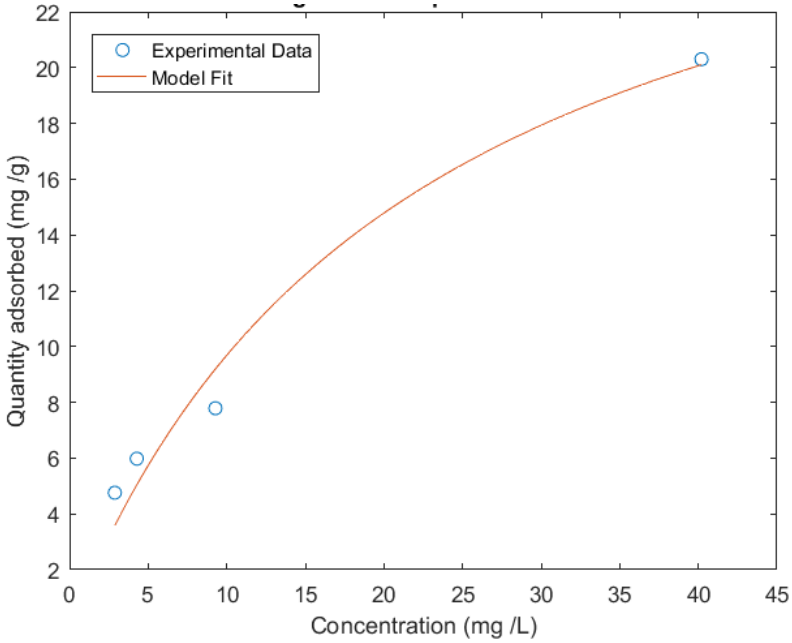

Figure 5.3: Langmuir adsorption model fit
GAC dose= 2.5-18.5 g.L^{-1}, time= 2 h, stirring speed= 200 RPM.

According to given regression coefficients, the adsorption equilibrium data highly complied with the Freundlich isotherm with a regression coefficient R^2 are as high as 99.93. The Freundlich constant (K_F) value of 2.366 suggests a relatively higher adsorption capacity compared to the Langmuir model. This indicates that the granulated wastewater possesses a high degree of surface heterogeneity and a significant number of adsorption

sites for TOC molecules. The Freundlich exponent (n) value of 1.72 suggests a slightly nonlinear adsorption behavior, indicating favorable adsorption at higher concentrations [32].

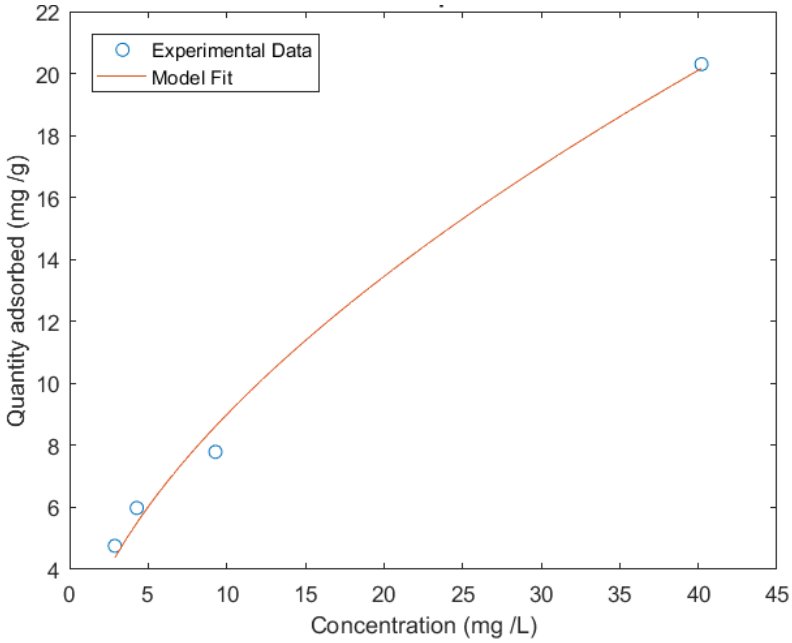

Figure 5.4: Freundlich adsorption model fit
GAC dose= 2.5-18.5 g.L^{-1}, time= 2 h, stirring speed= 200 RPM.

On the other hand, and through the Langmuir model, the maximum adsorption capacity (Q_m) of 31.21 mg.g^{-1} indicates that the GAC has a considerable number of adsorption sites available for TOC removal which were confirmed by the Langmuir constant (K_L) value of 0.46 L.mg^{-1} that suggests a moderate affinity between the TOC and the adsorbent material. The coefficient of determination R^2 value of 99.71% demonstrates a reasonably good fit of the Langmuir model to the experimental data. However, it may not necessarily mean that the adsorption process meets the requirements of the idealized localized monolayer model. In some cases the effect of nonhomogeneity of the surface may be compensated by adsorbate-adsorbent interactions and thus give rise to Langmuir plots [30].

Similar parameters were found in the work of Ananda J & al (2013) [41], where the adsorption of natural organic matter (NOM) from greywater on GAC was made. The commercial GAC showed a similar behavior in terms of maximum capacity Q_m and Freundlich adsorption intensity 1/n resulting in 29 mg.g^{-1} and 0.7, respectively.

Table 5.2: Isotherm models parameters for the adsorption of TOC on GAC

Isotherms	**Parameters**	**Values**
Langmuir	K_L ($L.mg^{-1}$)	0.46
	Q_m ($mg.g^{-1}$)	31.21
	R^2	99.71
Freundlich	K_F	2.36
	1/n	0.7
	R^2	99.93

5.2.2 GAC bed design through dynamic adsorption

5.2.2.1 Plot of breakthrough curve

To gain a deeper understanding of the adsorption kinetics and accurately describe the experimental data, the breakthrough curve in Figure 5.5, can be fitted using mathematical softawares.

This fitting process allows for the determination of adsorption parameters such as Q_m and k_1 which corresponds to 27.9 $mg.g^{-1}$ and 17.6, respectively. The maximum capacity found through this experimental setup was slightly lower than the capacity found through the Langmuir model (31.21 $mg.g^{-1}$).

As shown in this figure, the TOC concentration is reduced to its minimum concentration, once the solution is filtered through the depth of the adsorption column equals to the height of the mass transfer zone (HMTZ). In this case, there is no possibility of adsorption below the mass transfer zone. As the top layer of activated carbon column is saturated with adsorbate, the mass transfer zone moves down successively. The process is continued till the breakthrough is achieved [42]. The column breakthrough volume (V0.05, which is the volume that the effluent TOC concentration reaches approximately 5% of its initial concentration) and the column exhaustion volume (V0.95, which is the time that the effluent TOC concentration reaches approximately 95% of its initial concentration) are 1.95L and 7L, respectively.

In addition to this, the shape of the breakthrough curve depends on the nature of the pollutants; if the liquid contains nonabsorbable constituents, it would appear in the

effluent as soon as the carbon column is put into operation, which is why the curve doesn't start from the origin [42].

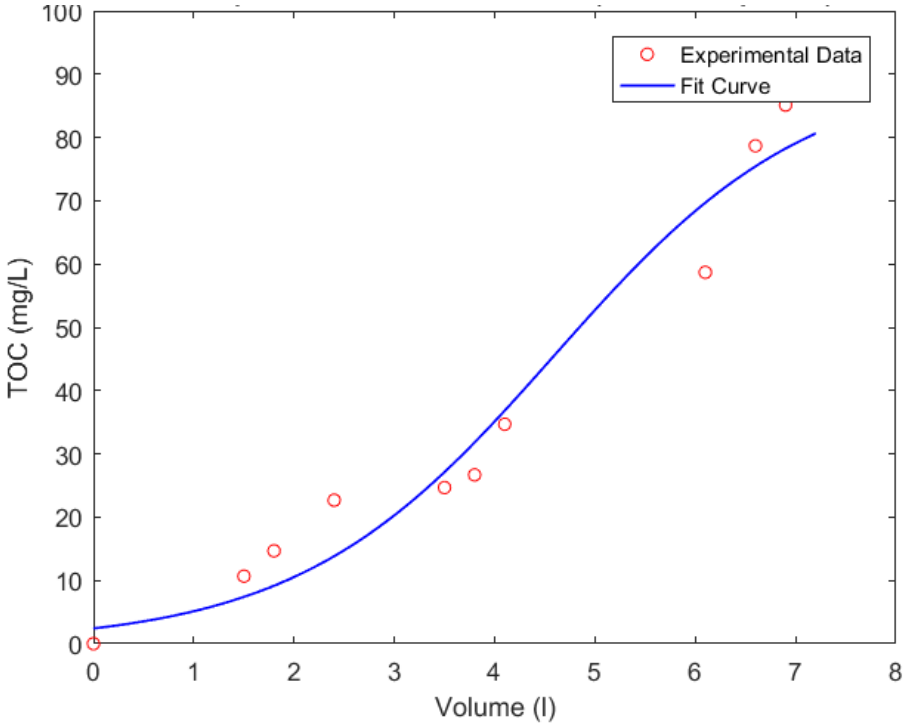

Figure 5.5: Breakthrough curve of TOC adsorption on GAC
GAC mass= 15 g, column diameter= 1 cm, bed depth= 24 cm , contact time= 8 s, flow rate= 30 ml.min^{-1}.

5.2.2.2 Design of full scale column using Thomas equation

As explained in section 4.2.3 , the design of a GAC bed is based on a scale up approach using Thomas equation. After the plot of the breakthrough curve and extracting the rate constant k_1 and the maximum capacity of the adsorption of TOC on GAC Q_m, the design of the bed knowing that the flow rate through this column is 100 m^3.h^{-1} is as follows:

1. The required GAC mass required in the full scale column (M_d) is calculated using thomas equation (Eq 4.9), the corresponding value is:

$$M_{\text{design}} = 4990\,\text{Kg} \approx 5000\,\text{Kg} \tag{5.1}$$

   Due to technical measurement, it would be more suitable to divide this mass and thus the flow into four columns. Therefore the GAC mass required in each column is:

$$M_{\text{design}} = 1250\,\text{Kg} \tag{5.2}$$

$$Q_{\text{design}} = 25\,\text{m}^3.\text{h}^{-1} \tag{5.3}$$

2. The volume and dimensions of the GAC bed: Empty bed volume(EBV_{design}): by applying equation 4.10:

$$EBV_{\text{design}} = \frac{1250\,\text{Kg}}{450\,\text{Kg/m}^3} = 2.78\,\text{m}^3 \approx 2.8\,\text{m}^3 \tag{5.4}$$

Cross-sectional area of the bed by applying equation 4.11:

$$A_{\text{design}} = \frac{25\,\text{m}^3/h}{15\,\text{m}/h} = 1.67\,\text{m}^2 \approx 1.7\,\text{m}^2 \tag{5.5}$$

Diameter of the bed by applying equation 4.12:

$$d_{\text{design}} = \sqrt{\frac{4 \cdot 1.67m^2}{\pi}} = 1.45\,\text{m} \tag{5.6}$$

Depth of the bed by applying equation 4.13:

$$D_{\text{design}} = \frac{2.78\,\text{m}^3}{1.67\,\text{m}^2} = 1.66\,\text{m} \approx 1.7\,\text{m} \tag{5.7}$$

3. The liquid flow rate per unit by applying equation 4.14:

$$q_{B,\text{design}} = \frac{25\,\text{m}^3/h}{2.78\,\text{m}^3} = 9\,\text{h}^{-1} \tag{5.8}$$

4. The service time using equation 4.15:

$$t_{B,\text{design}} = \frac{2000\,\text{m}^3}{25\,\text{m}^3/\text{h}} = 80\,\text{h} \tag{5.9}$$

$$t_{\text{B,design}} = 3.33\,\text{d} \approx 4\,\text{d} \tag{5.10}$$

To attest the column design calculations, it is essential to compare them to typical design values for GAC contactors summerized in Table 5.3.

The calculated value of 2.8 m^3 is notably lower than the typical range of 5-25 m^3. This discrepancy indicates that the GAC column may have a smaller void space than what is typically recommended. The bed depth to diameter ratio is calculated as 1.2, indicating

a moderate ratio between the two parameters. This value falls within the typical range of 1.0-2.5, suggesting a reasonable design choice that should provide sufficient contact time for effective contaminant removal. However, a notable discrepancy arises in the service time parameter. The calculated value of 4 days significantly deviates from the typical range of 50-100 days, this may be due to the high polluants load that is present in the effluent, therefore the adsorption of the TOC onto the GAC was hampered, thus the service time is lower than the typical value.

Table 5.3: Comparison between the calculated values and typical design values for GAC contactors

Parameter	Unit	Calculated value	Typical value [42]
Volumetric flow rate	m^3	25	25-200
Empty bed volume	m^3	***2.8***	5-25
Cross sectional area	m^2	***1.7***	2.5-15
Bed depth	m	1.7	0.9-2
Bed depth to diameter ration	$m.m^{-1}$	1.2	1.0-2.5
Void fraction	$m^{-3}.m^{-3}$	0.4	0.38-0.42
GAC density	$kg.m^{-3}$	450	350-650
Service time	d	***4***	50-100
Velocity approach	$m.h^{-1}$	15	5-15

5.2.3 Pretreatment on activated carbon test

The presented Table 5.4 provides the characteristics of wastewater after treatment with granular activated carbon , along with the corresponding removal rates.

Table 5.4: Pretreated on GAC wastewater characteristics

Parameter	**Unit**	**Value**	**Removal rate %**
Phenols	$mg.L^{-1}$	0.0	100
TN	$mg.L^{-1}$	0.7	96.64
Turbidity	NTU	1.12	96.6
TSS	$mg.L^{-1}$	3	96.2
TOC	$mg.L^{-1}$	4.02	95.6
BOD_5	$mg.L^{-1}$	15	90
COD	$mg.L^{-1}$	16	85.58
Chloride	$mg.L^{-1}$	11.9	46.29
Iron	$mg.L^{-1}$	0.50	41.17
Cyanide	$mg.L^{-1}$	0.23	20.68
Conductivity	$mS.cm^{-1}$	2.02	4.7
TH	$mg_{CaCO3}.L^{-1}$	89.7	2.07
Sodium	$mg.L^{-1}$	410.3	1.37
CaH	$mg_{CaCO3}.L^{-1}$	59.6	1.16
TAT	$mg.L^{-1}$	100	/
pH	/	7.02	/
Silica	$mg.L^{-1}$	0.013	/
Lead	$mg.L^{-1}$	0.00	/
Zinc	$mg.L^{-1}$	0	/

The results demonstrate the effectiveness of GAC in removing organic pollutants, as evidenced by the significant high rate removal such 100%, 95.6% and 85.58% of phenols, TOC and COD, respecively.

Furthermore, the decrease in total suspended solids is indicative of the ability of GAC to remove solid particles and colloidal matter from the wastewater. The high removal rate of TSS which is 96.2% underscores the efficient filtration properties of GAC, resulting in a cleaner water.

Regarding the mineral constituents, such as sodium and chloride, their relatively decreased concentrations in the treated wastewater result in a slightly lower conductivity value. Therefore, The GAC treatment process likely involves the adsorption of these ions onto the carbon surface since the activated carbon is inert.

5.3 Deminiralization using electrodialysis

5.3.1 Determination of limiting current

The limiting current value for the initial solution conductivity of 2.02 $\mu S\, cm^{-1}$ is found to be 0,14 A, as illustrated in Figure 5.6. The plateau observed in the curve corresponds to a total concentration polarization in the diffusion layer near the membrane. The optimal current, corresponding to 80% of the limiting current, can be determined using Equation 5.11.

$$I_{optimal} = 0,8\, I_{lim} = 0,12\, A \tag{5.11}$$

The simplified equation derived from Ilkovic's law $I_{lim} = KC_f$, underscores the direct influence of the ionic concentration of the diluent solution on the limiting current. Consequently, a lower concentration results in a reduced limiting current. In order to achieve the desired low final conductivity of the diluent, it is imperative to conduct all electrodialysis experiments with a current value set below the optimal current.

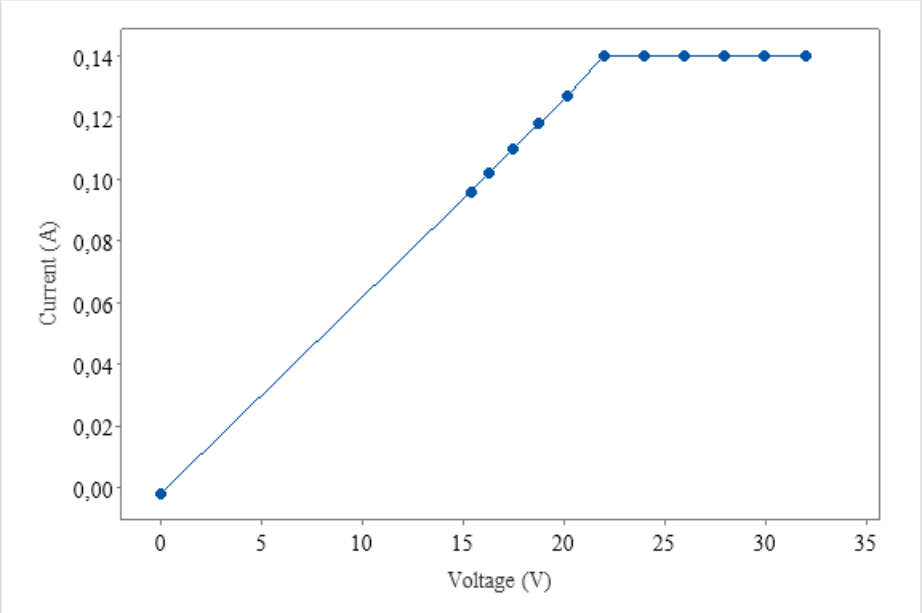

Figure 5.6: Polarization curve. *(σ_0 = 2,02 $\mu S\, cm^{-1}$, Flux rate 25 L h^{-1}, pH = 7, $[NaCl]_c = 1g\, L^{-1}$)*

5.3.2 Preliminary studies

Current (I) : The time required to maintain a constant current at the stack terminals is longer when working with low currents as shown in Figure 5.7, which is desirable for making necessary adjustments and maintaining a constant current factor during the execution of experimental plan and for the determination of optimized values . Moreover, working in constant current mode helps reduce the risk of membrane polarization. Polarization can occur when the current varies abruptly, leading to a decrease in the efficiency of the ion exchange process. By maintaining a constant current, polarization is minimized, thereby maximizing the performance of electrodialysis.

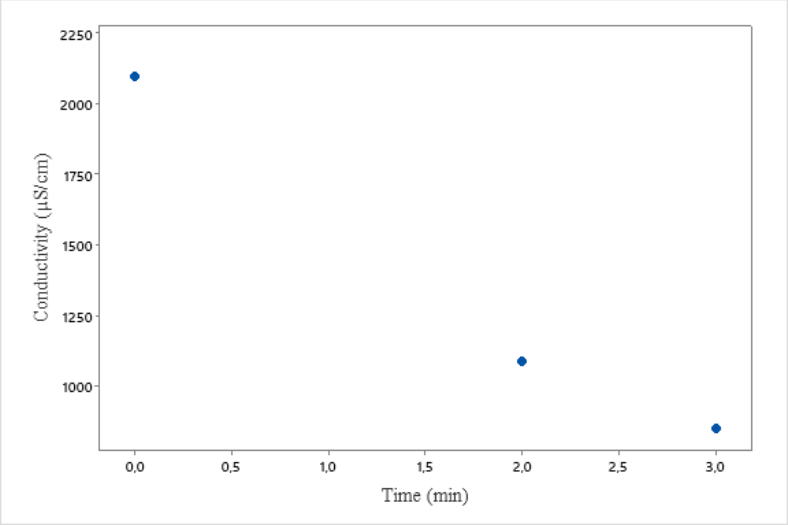

(a) I=0,11 A

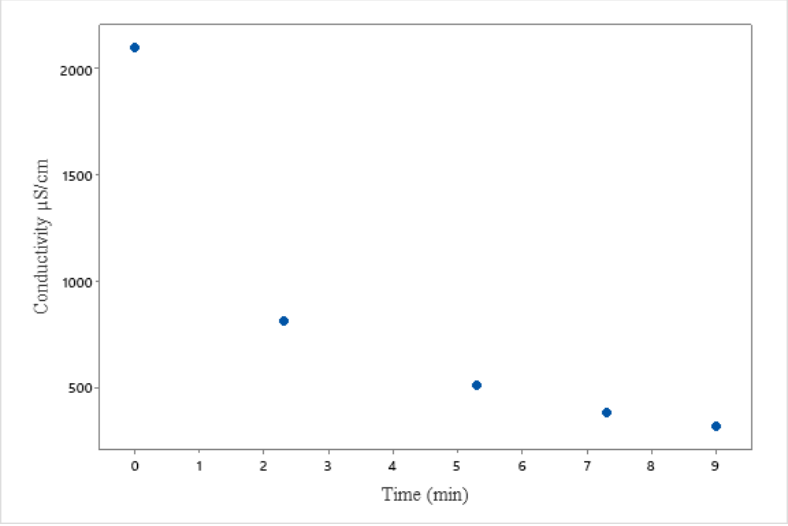

(b) I=0,08 A

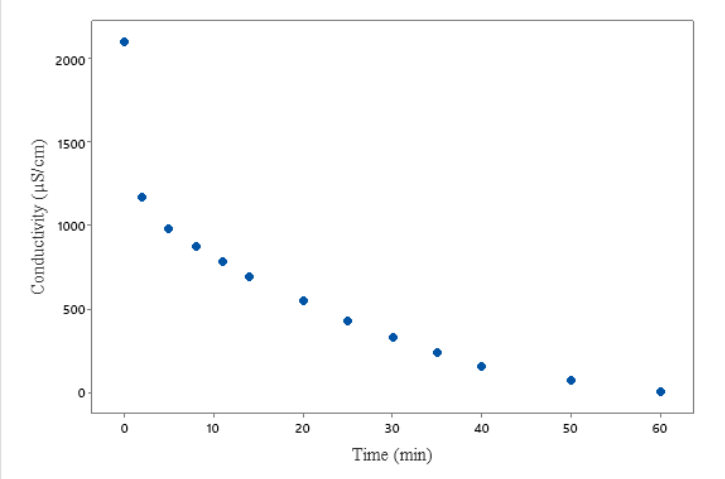

(c) I=0,02 A

Figure 5.7: Influence of current on the conductivity of the diluent solution over time. $\sigma_0 = 2{,}02\ \mu S\, cm^{-1}$, *Flux rate 25 L* h^{-1}, $pH = 7$, $[NaCl]_c = 1 g L^{-1}$

pH: Considering the measured pH values obtained from the refinery effluent database, it has been determined that the acceptable pH range for the process is between 7 and 10. It is crucial to ensure that the pH of the effluent remains within this range in order to comply with the required standards, regulations and in order to avoid the need for costly additive injections

Concentrate solution: A fixed concentration of 1 mg l^{-1} is recommended ($\sigma_{NaCl} \leq \sigma_D$) to achieve the desired increase in conductivity and ensure optimal performance of the system. Table 5.5 summarized the values of factors.

Table 5.5: Factors studied and their levels

Coded variables	Factors	Min	Max
A	I : Current (A)	0,04	0,08
B	[NaCl] (mg L^{-1}) in concentrate compartment	0,6	1
C	pH of feed water	7	10

Table 5.6: Experimental matrix given by the Box-Behnken Design (BBD)

	Coded variable			Natural variable		Responses			
RunOrd	A	B	C	I (A)	$[NaCl]_c$	pH	σ_D ($\mu S\ cm^-1$)	Steady time (min)	Removal rate %
1	-1	-1	0	0,04	0,6	8,5	33	47	98
2	1	-1	0	0,08	0,6	8,5	326	15	84
3	-1	1	0	0,04	1	8,5	29	40	99
4	1	1	0	0,08	1	8,5	300	18,5	85
5	-1	0	-1	0,04	0,8	7	37	40,5	98
6	1	0	-1	0,08	0,8	7	400	13	80
7	-1	0	1	0,04	0,8	10	80	39	96
8	1	0	1	0,08	0,8	10	302	15,5	85
9	0	-1	-1	0,06	0,6	7	147	22,5	93
10	0	1	-1	0,06	1	7	102	26,5	95
11	0	-1	1	0,06	0,6	10	130	23,5	94
12	0	1	1	0,06	1	10	179	24	91
13	0	0	0	0,06	0,8	8,5	242	18	88
14	0	0	0	0,06	0,8	8,5	245	17,5	88
15	0	0	0	0,06	0,8	8,5	247	19	88

5.3.3 Box-Behnken statistical analysis of demineralization rate and time responses

Diagnostics of the model

The residuals of both responses form a random pattern and relatively flat band around the residual = 0 line. There are no noticeable outliers as shown in Figures 5.8 and 5.9.

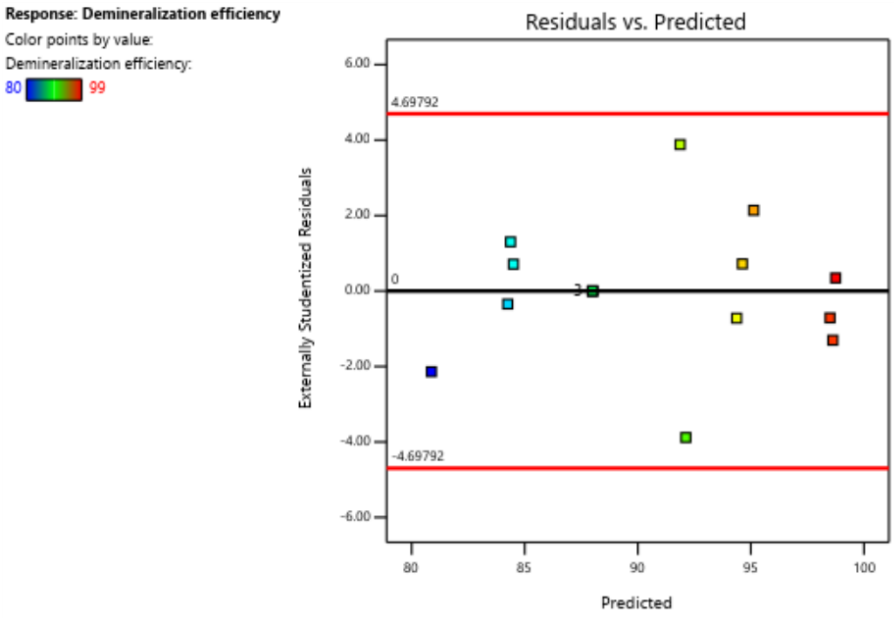

Figure 5.8: Residuals vs predicted values for demineralization rate model

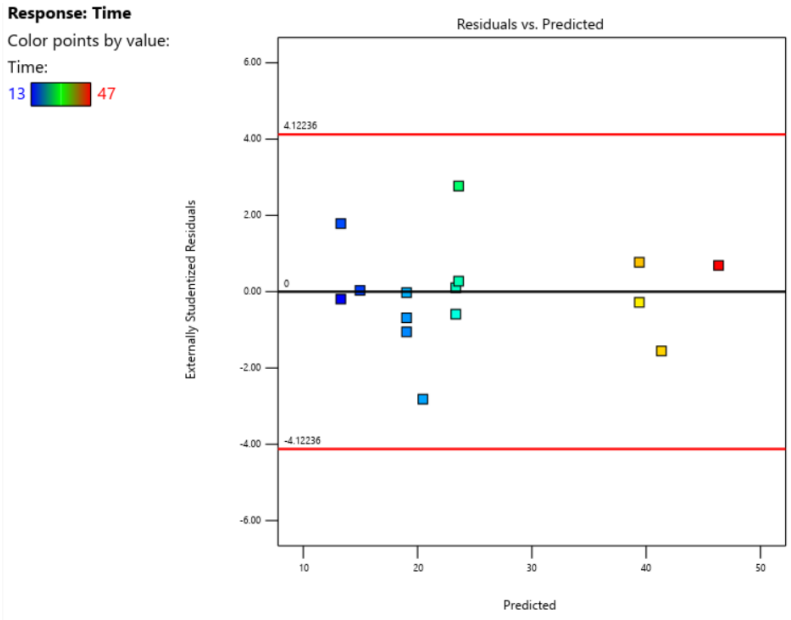

Figure 5.9: Residuals vs predicted values for steady time model

The normality of the residuals is determined by evaluating the normal probability plot Figures 5.10 and 5.11, The data points are close to the line, indicating that the sample distribution is close to the theoretical distribution and that the RSM model is adequate.

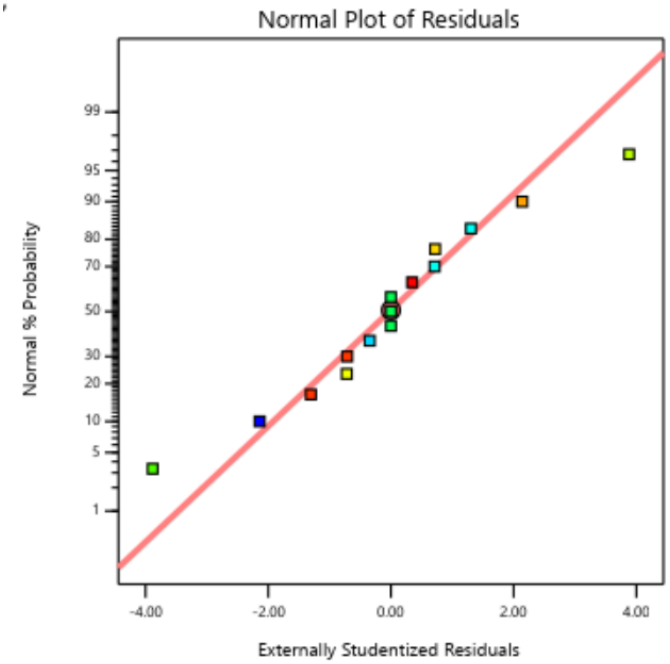

Figure 5.10: Normal plot of demineralization rate response residuals

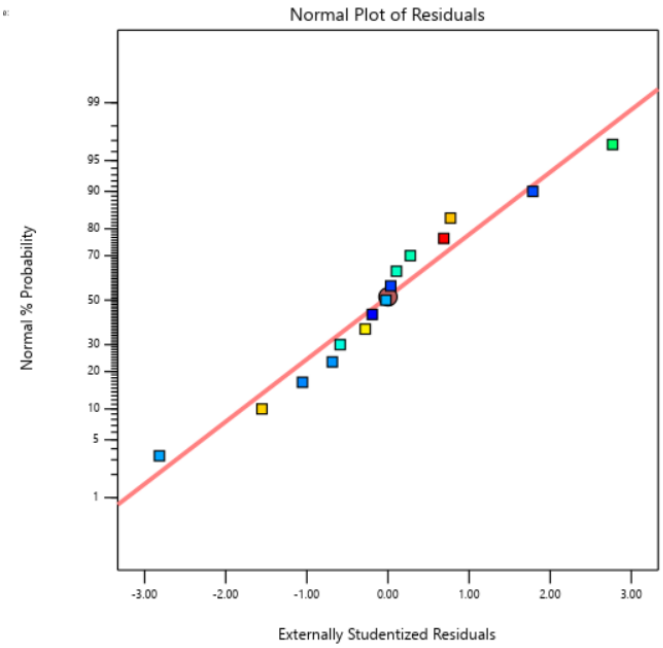

Figure 5.11: Normal plot of steady time response residuals

Figures 5.12 and 5.13 show the relationship between the actual and predicted values of Y. A good agreement is observed.

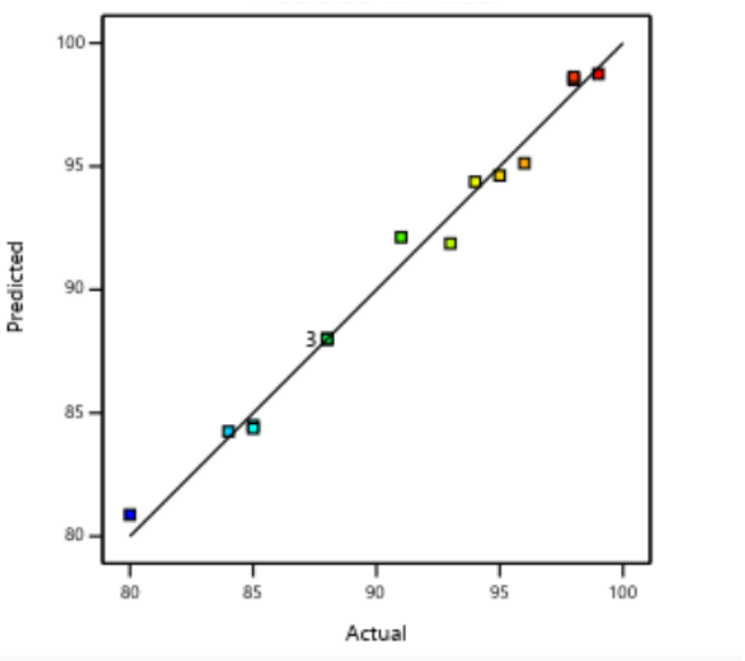

Figure 5.12: Predicted vs Actual values for demineralization rate response

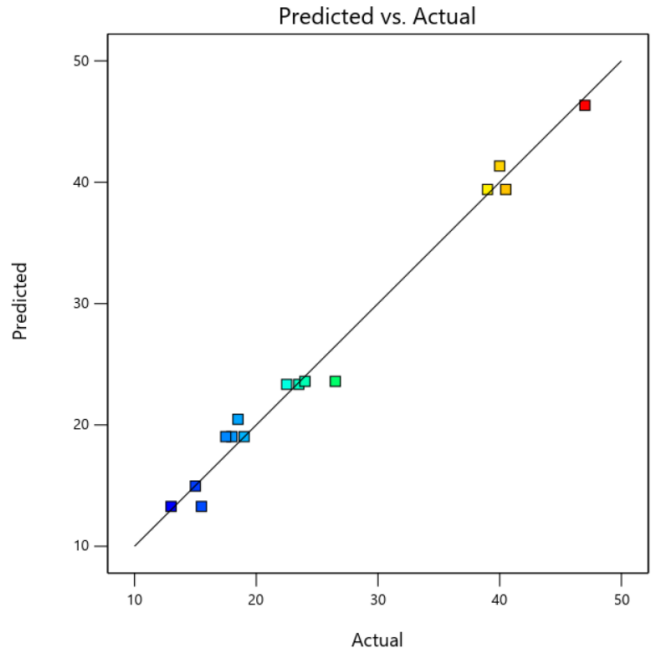

Figure 5.13: Actual vs Predicted values for steady time response

Analysis of variance ANOVA

Table 5.7 and 5.8 relatives to the analysis of variance for demineralization efficiency and steady time show that the two models are significant i.e. The results are not due to

chance; they reflect a significant correlation with reality. P-values less than 0.05 indicate model terms are significant. In this case (A, B, C, AC, BC, B^2, C^2)(A, B, AB, A^2, B^2) are the significant model terms respectively.

Table 5.7: ANOVA for demineralization efficiency quadratic model

Source	Sum of Squares	df	Mean Square	F-value	p-value	
Model	478.65	9	53.18	46.25	0.0003	significant
A-I	406.13	1	406.13	353.15	< 0.0001	
B-[Nacl]	0.1250	1	0.1250	0.1087	0.7550	
C-pH	0.0000	1	0.0000	0.0000	1.0000	
AB	0.0000	1	0.0000	0.0000	1.0000	
AC	12.25	1	12.25	10.65	0.0224	
BC	6.25	1	6.25	5.43	0.0671	
A^2	0.0000	1	0.0000	0.0000	1.0000	
B^2	45.23	1	45.23	39.33	0.0015	
C^2	11.31	1	11.31	9.83	0.0258	
Residual	5.75	5	1.15			
Lack of Fit	5.75	3	1.92			
Pure Error	0.0000	2	0.0000			
Cor Total	484.40	14				

Table 5.8: ANOVA for steady time efficiency quadratic model

Source	Sum of Squares	df	Mean Square	F-value	p-value	
Model	1662.67	9	184.74	86.09	< 0.0001	significant
A-I	1365.03	1	1365.03	636.13	< 0.0001	
B-[Nacl]	0.1250	1	0.1250	0.0583	0.8189	
C-pH	0.0312	1	0.0312	0.0146	0.9086	
AB	27.56	1	27.56	12.84	0.0158	
AC	4.00	1	4.00	1.86	0.2304	
BC	3.06	1	3.06	1.43	0.2858	
A^2	203.10	1	203.10	94.65	0.0002	
B^2	76.16	1	76.16	35.49	0.0019	
C^2	7.41	1	7.41	3.45	0.1222	
Residual	10.73	5	2.15			
Lack of Fit	9.56	3	3.19	5.46	0.1586	not significant
Pure Error	1.17	2	0.5833			
Cor Total	1673.40	14				

Models equations

The regression equations in coded units after removing the terms that are not significant (model reduction) are as follow :

$$\text{Removal rate} = 88 - 7,13A + 0,125B + 3,5BB + 1,75CC + 1,75AC - 1.25BC \quad (5.12)$$

$$\text{Steady time} = 19,04 - 13,06A + 0,1250B + 2,63AB + 7,31A^2 + 4.43B^2 \quad (5.13)$$

Table 5.9: Fit statistics of demineralization rate and steady time models

Fit statistics	Demineralization rate (%)	Steady time
R^2	0.9881	0.9849
Adjusted R^2	0.9763	0.9765
Predicted R^2	0.8841	0.9379
Adeq Precision	27.0061	31.2160

- The predicted R^2 is in reasonable agreement with the Adjusted R^2 ; i.e. the difference is less than 0,2. indicating that the RSM model is suitable for the data range investigated in this study.
- Adeq Precision measures the signal to noise ratio. A ratio greater than 4 is desirable. The ratio of 27 and 31,21 indicates an adequate signal. This model can be used to navigate the design space.

5.3.3.1 Removal rate response surface plots

The predicted results are visualized through 3D response surface plots to illustrate the effects and interactions.

Figure 5.14 illustrates the relationship between demineralization efficiency, pH and applied current. It shows that a current of 0,04 A results in high demineralization efficiency, whereas higher currents lead to lower efficiency.

- for I = 0,08 and the pH increase, indicating the addition of OH^- ions, has a negative effect within the center of the pH domain (pH=8,5), which corresponds to a minimum efficiency. At pH=10, the efficiency is slightly higher compared to the neutral solution.
- The opposite effect is observed when 0,04 A is used, the efficiency does not stop decreasing until it reaches a value of 96%.

In the ED process, At the start of the experiments, the conductivity is high, and the resistance is low; therefore, the ion migration is speed and accompanied by a fast demineralization speed of the dilute [43]. The resistance continues to increase, in addition the constraints of the DC supply's maximum voltage (32 V) resulting in decreasing

courant. Therefore, when the current is approximately 0,08 A, the resident time of the solution during treatment is short, resulting in a lower demineralization removal efficiency.

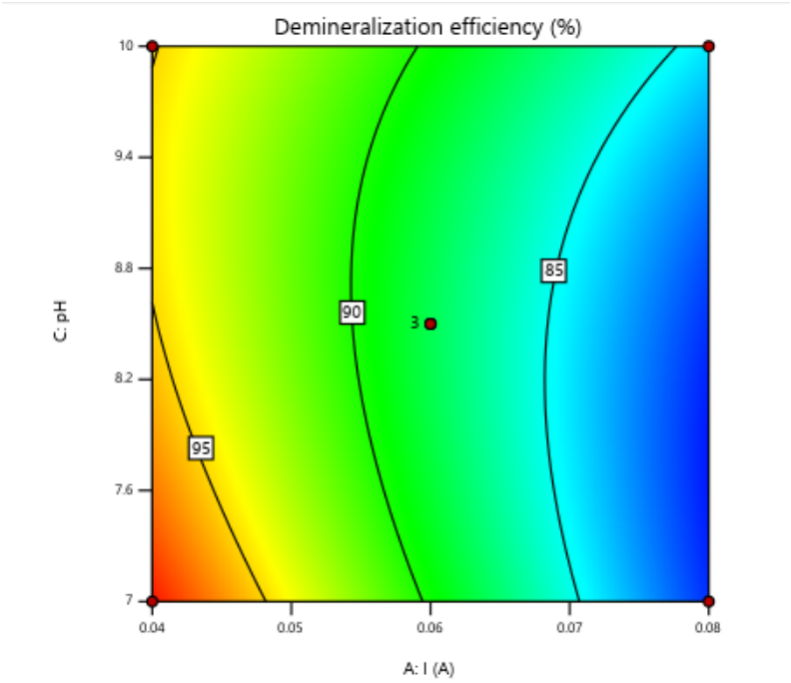

(a)

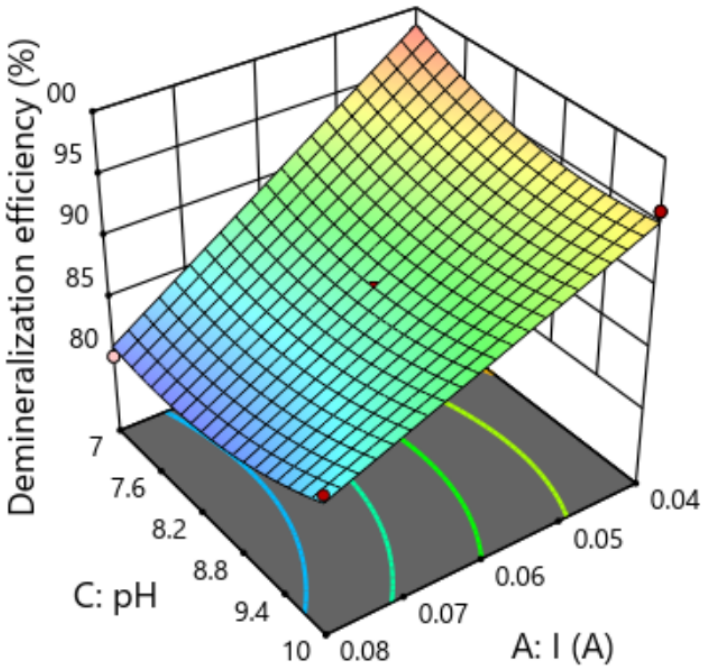

(b)

Figure 5.14: a- Contour plot, b- surface response of Current-pH

The figures 5.16 and 5.15 illustrate the removal rate response in function of NaCl concentration in the concentrate compartment and pH. The conductivity response surface exhibits symmetry around its center, representing the lowest value. Both the pH of the effluent and the concentration of NaCl have a similar effect on ions removal. As we move from the lower to the center level, the demineralization rate decreases, and then it starts to increase again.
In this case, the combination of extreme levels of pH and NaCl concentration can lead to optimum efficiency in the electrodialysis process. The pH level affects the ionization state of the solutes, while the NaCl concentration influences the conductivity and ion transport across the membranes.

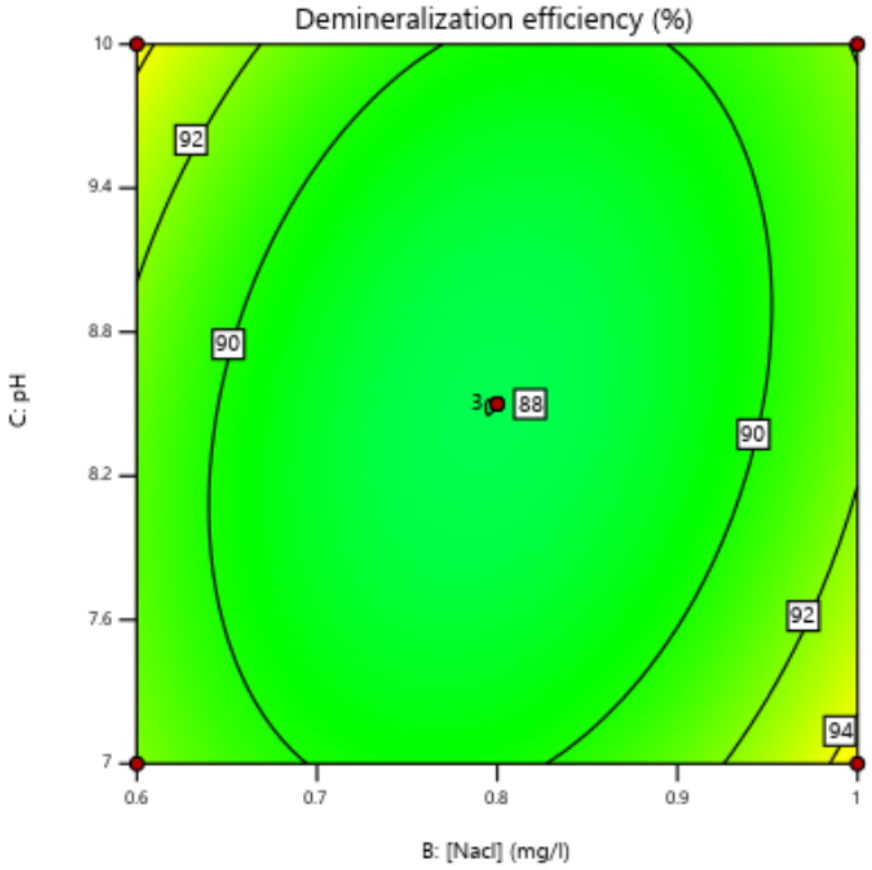

Figure 5.15: Contour plot of [NaCl]-pH

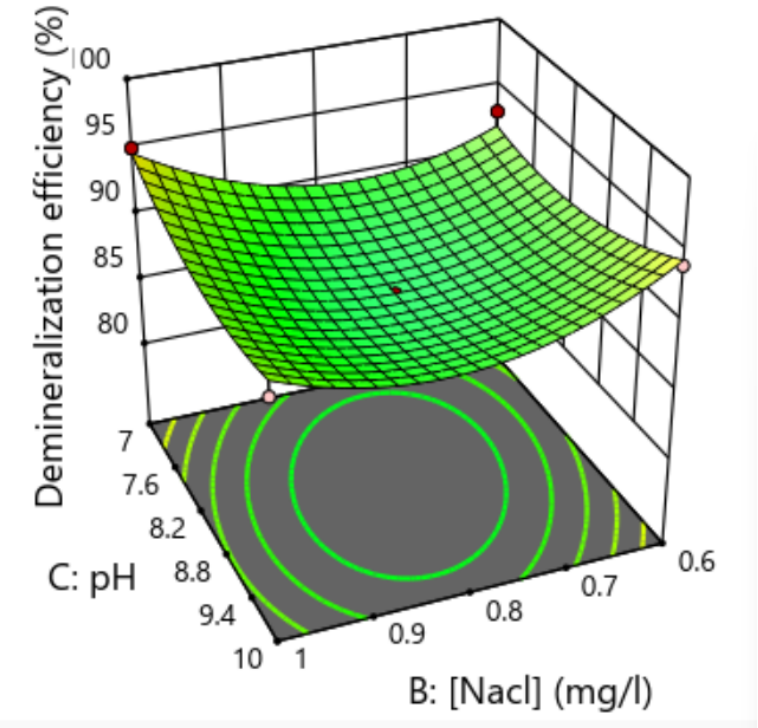

Figure 5.16: Surface response of [NaCl]-pH

Steady time response surface plots

Figure 5.17 illustrates the relationship between time and the significant interaction term of the model, [NaCl]-current. The time response exhibits a similar behavior to the demineralization rate, where the time required to maintain treatment at a constant current decreases as the current ranges from 0.04 to 0.08 A.

The minimum time response is observed at the center level of [NaCl] when the applied current was low, indicating that the lowest current tends to favor the lowest concentration of [NaCl] at 0,6 g l^{-1}, while higher currents tend to favor the higher concentrations. For example, at (I, [NaCl]) = (0,04, 0,6), the response time reaches its maximum at 47 minutes comparing (0,04, 1). On the other hand, when considering (0,08, 1), the time is 18.5 minutes, indicating a longer duration for the treatment process compared to (0,08, 0,6).

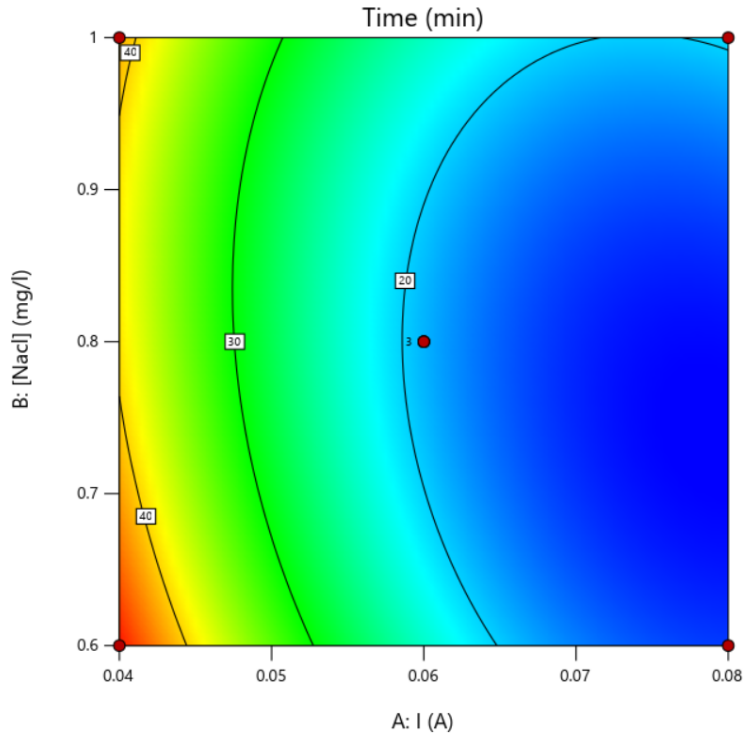

(a)

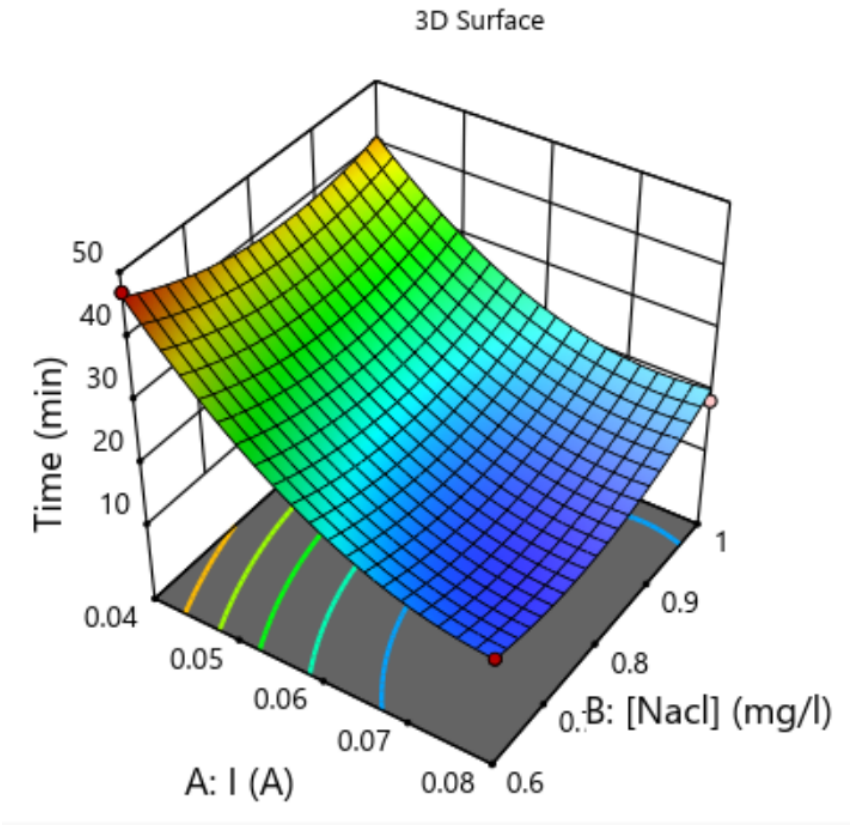

(b)

Figure 5.17: a- Contour plot, b- surface response of I-[NaCl]

By solving Equations 5.13 and 5.12, the optimal values of the applied current, [NaCl] in the concentrate compartment, and pH were determined to be 0,06 A, 1 g l^{-1}, and 7, respectively. According to the software prediction, under these optimal conditions, the removal of ions is expected to reach 94,62%. Table 5.10 presents the experimental and optimal values of the model equation for two test experiments. It is evident from the table that the predicted values of the model closely match the experimental values in the tests.

Table 5.10: The results of the confirmatory tests of the proposed model for demineralization efficiency and steady time by ED

Expe	current (A)	[NaCl] (g l^{-1})	pH	Steady time	σ_D ($\mu S\ cm^{-1}$)	Removal rate (%)
1	0,06	1	7	23,5	130	93,5
2	0,06	1	7	23,8	121	94
opt	***0,06***	***1***	***7***	***23,5***	***110,413***	***94***

Desirability function

The first column of the graph indicates the response values at each level of applied current, [NaCl], and pH. The current variable parameters are set to their optimal values as shown in figure 5.18. The objective was to minimize conductivity and time. The predicted values are 110,41 $\mu S\ cm^{-1}$ and 23,5 min , respectively, which correspond to a desirability of 0,733.

The following observations can be made:

- Current: The current has a significant effect on both responses. The optimal parameter value is in the middle of the range (0,06), which represents a compromise between conflicting objectives.
- NaCl concentration: The optimal NaCl parameters are at the maximum levels during experimentation. This result suggests using higher concentrations for experimentation. the resulting effect on conductivity is the opposite of the effect on time.
- pH: The optimal pH parameters are at the minimum levels during experimentation. This result suggests using lower pH for experimentation.

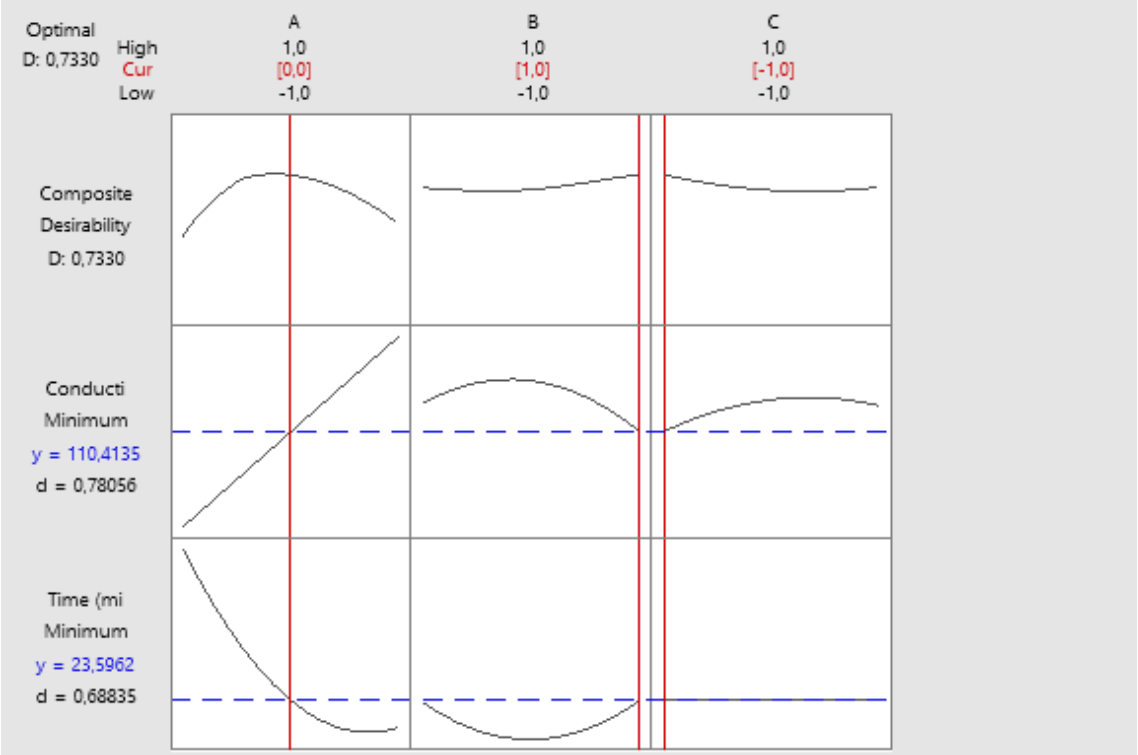

Figure 5.18: Optimisation diagram for conductivity and time

5.4 Cation and anion demineralizer design

A hydrogen cation and strong base anion exchanger system are designed for polishing water treated by ED. The flow is 100 $m^3 d^{-1}$. the volumetric exchange capacities of cationic and anionic resins are 127,3 kg $CaCO_3\, m^{-3}$ and 350 kg $CaCO_3\, m^{-3}$, respectively. To determine the volume and dimensions of both exchangers we compute the total cations and anions in mg l^{-1} as $CaCO_3$ as shown in table 5.11. The regeneration cycle is 4 days.

Table 5.11: The ions concentrations in water treated by electrodialysis (ED) before entering the resin bed

ion	$[M^+]$			ion	$[M^-]$		
	g L^{-1}	meq g^{-1}	mg L^{-1} as $CaCO_3$		g L^{-1}	meq g^{-1}	mg L^{-1} as $CaCO_3$
Na^+	20,25	0,88	44,02	Cl^-	18,11	0,51	25,54
Ca^{2+}	0	0	0	HCO^{3-}	0	0	0
Mg^{2+}	0	0	0	-	-	-	-
Totale	-	0,88	44,02		-	0,51	25,54

Hydrogen cation exchangers

The volume of resin required :

$$V_{RC} = \frac{100\,24\,4\,44,02}{350} = 1,2\,m^3 cycle^{-1} \tag{5.14}$$

$$\text{resin depth} = \frac{1,2 * 1,5}{\pi\,0,5^2} = 2,3\,m \tag{5.15}$$

Anion exchange resin

The volume of resin required :

$$V_{RA} = \frac{100\,24\,4\,127,3}{127,3} = 1,92\,m^3\,cycle^{-1} \tag{5.16}$$

$$\text{resin depth} = \frac{1,92 * 1,5}{\pi\,0,5^2} = 2,8\,m \tag{5.17}$$

In practical applications, the small bench column was utilized, at the same masse (10 g), to facilitate the reduction of pollutant concentrations in the effluent, and because of Sodium (Na^+), Chloride (Cl^-), Calcium (Ca^{+2}), Hydrogen ion (H^+), and Hydroxyl ion (OH^-) are adsorbed well by the resin. The achieved concentrations, close to zero for most pollutants are summarized in Table 5.12 as well as the water aspect shown in Figure 5.19.

Figure 5.19: Raw wastewater and final demineralized water

Final demineralized water characteristics

Table 5.12: Final ions concentration in treated water

Parameter	Unit	Value
Turbidity	NTU	0,8
TSS	g L^{-1}	0
TOC	g L^{-1}	0
Chloride	g L^{-1}	2,9
Iron	0	0
Conductivity	$\mu S\ cm^{-1}$	20
TH	g $CaCO_3$ L^{-1}	0
Sodium	g L^{-1}	1,5
TAT	g $CaCO_3$ L^{-1}	0
pH	-	6,3
Silica	g L^{-1}	0,06
Zinc	g L^{-1}	0

5.5 Demineralization trials using Electrodeionization

5.5.1 Mode determination of limiting current-deionization

The curve presented in the Figure 5.20 can be interpreted as a current zone, similar to the faradaic region of a typical electrochemical curve before reaching the critical current. [44]

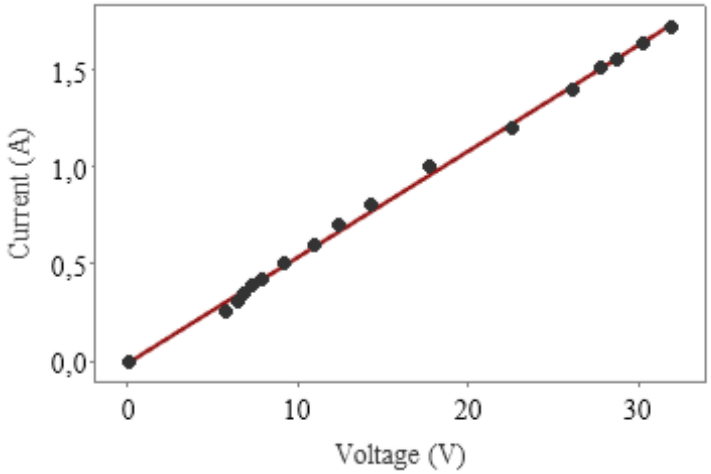

Figure 5.20: EDI Polarization curve. *(σ_{D0} = 828 $\mu S\,cm^{-1}$, Flux rate 100 L h^{-1}, pH = 7, σ_{NaCl} = 541 $\mu S\,cm^{-1}$)*

The water recovered through the dilute compartment exhibits a favorable yield in the electro-deionization process. When a current density of 60 mA is applied, after 30 min the obtained water has a conductivity of 571 $\mu S\ cm^{-1}$ (see Figure 5.21), corresponding to a 31% reduction in ion concentration as shown in Figure 5.22. However, An initial conductivity of the neutral industrial effluent, which contains ions such as Mg^{2+}, Zn^{2+}, SO_4^{2-}, is 950 $\mu S\ cm^{-1}$. After a treatment using EDI with a current density of 40 mA cm^{-2} applied for 30 minutes, the conductivity of the water decreases to 300 $\mu S\ cm^{-1}$ [45]. As shown in Figure 5.22, The evaluation of the EDI system performance does not require a long duration. The demineralization rate increases rapidly within the first 10 minutes and then it achieves a steady state, primarily due to the early protonation of the resin. In the second stage as a result of the rapid loading of the resins [46].

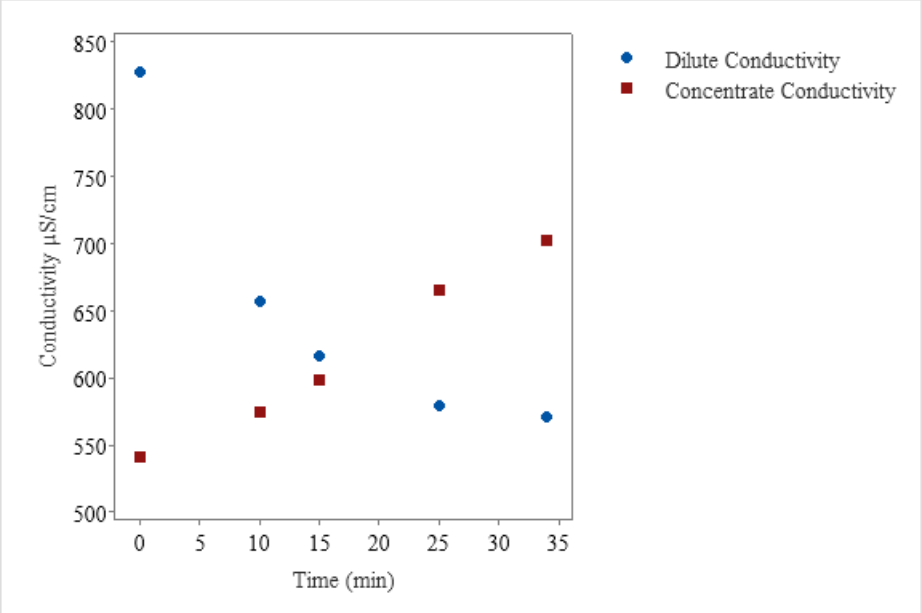

Figure 5.21: Dilute, concentrate conductivity versus time *($\sigma_{D0} = 828\ \mu S\,cm^{-1}, \sigma_{C0} = 541\ \mu S\,cm^{-1}$, Flux rate 100 L h^{-1}, pH = 7)*

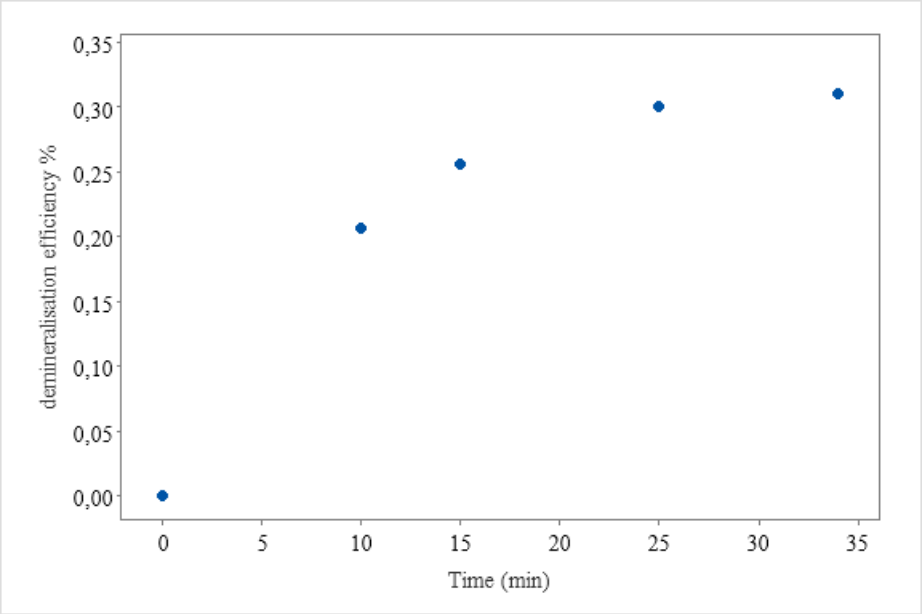

Figure 5.22: Demineralisation efficiency versus time *($\sigma_{D0} = 828\ \mu S\,cm^{-1}$, $\sigma_{C0} = 541\ \mu S\,cm^{-1}$, Flux rate 100 L h^{-1}, pH = 7)*

General conclusion and perspectives

This study presents an opportunity for the reuse of the liquid effluent from Algiers Refinery as makeup water for a medium-pressure boiler.

To contextualize this work, initially, the different possibilities of reuse, along with their benefits, requirements, and limitations were presented. The physical and chemical characteristics of the effluent showed high concentrations of contaminants. Therefore, a series of treatment studies were conducted, beginning with adsorption on activated carbon in order to remove organic matter. Next, the optimization of electrodialysis parameters for the demineralization process, including applied current, concentrate solution, and pH, were investigated.

Lastly, a polishing treatment using resin was employed. The combination of electrodialysis and resin was investigated by implementing a laboratory-scale electrodeionization device.

The proposed study methodology demonstrated the effectiveness of the GAC bed in removing organic pollutants, 100% for phenols, 95,6% for TOC, and 85,58% for COD, and achieving high removal efficiencies of suspended solids, and turbidity. The adsorption process for complex mixtures . Furthermore, the optimization of electrodialysis parameters using the Box-Behnken design enabled the prediction of optimal conditions for achieving high demineralisation rates (94%) within the shortest possible time (23,5 min). The optimal parameter values that were determined are as follows :

- Applied current: 0,06 A,
- Concentrate solution : 1 g l^{-1} of NaCl,
- pH = 7.

The advantage of the design is its ability to operate within the safe zone of the domain, minimizing the potential risk of polarization, fouling, and reduced current efficiency. After the water was treated by electrodialysis, it was introduced into a bench-scale resin-mixed bed. The concentration of TH, TAC, Na^+, Cl^-, and silica in the treated water were reduced to zero. the final conductivity of treated wastewater is found to be equal to 20 $\mu S\ cm^{-1}$. The demineralization treatment appears effective as it eliminated pollutants of concern like alkalinity and silica that can cause calcium deposits. However, further treatment is needed to reach the desired conductivity of 0.02 $\mu S\ cm^{-1}$. On the other hand, electrodeionization demonstrates reliable demineralization with a removal efficiency of 31% achieved within a 30-minute duration. EDI shows promising results By incorporating resin into the electrodialysis, ion migration is enhanced even when working with very

dilute solutions. From economical point of view, EDI is economically interesting as a replacement of existing ion exchange beds.

In relation to the objective of this work, the results enabled us to establish the specifications to be achieved during the pre-treatment, electrodialysis, and resin stages to produce boiler feed water. As a recommendation for future research, conduct a bacteriological analysis of the wastewater to assess bacterial contamination and consider chlorination treatment if necessary before using the WW on GAC. Also, use a bigger apparatus for dynamic adsorption of TOC on GAC to replicate real-world conditions accurately and obtain more representative results; and finally, implement effective GAC regeneration techniques to extend its lifespan and optimize resource utilization.

On the other hand, it is suggested to continue the development and comparison of conventional electrodialysis (ED) with electrodeionization (EDI) in terms of their performance and properties, especially the electrochemical regeneration. By conducting comparative studies, a better understanding can be gained regarding the advantages and limitations of each technique, ultimately leading to improvements in the treatment for pure water. Investigate the scalability of the developed methodology and assess its feasibility for large-scale implementation in industrial settings. Conduct pilot-scale experiments and economic assessments to evaluate the cost-effectiveness and practicality of the proposed approach.

Bibliography

[1] Wastewater as a resource. 5 2022.

[2] Metcalf Eddy Inc. An Aecom Company, Takashi Asano, Metcalf Eddy, Franklin L. Burton, Harold L. Leverenz, Ryujiro Tsuchihashi, and George Tchobanoglous. *Water Reuse*. McGraw Hill Professional, 1 2007.

[3] National Research Council, Division On Earth Studies, Life, Water Science Board, Technology, and Committee On The Assessment Of Water Reuse As An Approach To Meeting Future Water Supply Needs. *Water Reuse*. National Academies Press, 7 2012.

[4] George Tchobanoglous, Franklin Louis Burton, H. David Stensel, and Metcalf Eddy Inc. *Wastewater Engineering: Treatment and Reuse*. McGraw-Hill Science/Engineering/Math, 1 2003.

[5] Mohammed Saedi Jami, Mutiu K. Amosa, Ma An Fahmi Rashid Al-Khatib, Dzun Noraini Jimat, and Suleyman Aremu Muyibi. Boiler-Feed and Process Water Reclamation from Biotreated Palm Oil Mill Effluent (BPOME): A Developmental Review. *Chemical and Biochemical Engineering Quarterly*, 27(4):477–489, 12 2013.

[6] Syed R. Qasim and Guang Zhu. *Wastewater Treatment and Reuse Theory and Design Examples, Volume 2:*. CRC Press, 11 2017.

[7] Juan M. Lema and Sonia Suarez Martinez. *Innovative Wastewater Treatment Resource Recovery Technologies: Impacts on Energy, Economy and Environment*. IWA Publishing, 6 2017.

[8] Nader Al-Bastaki and Abderrahim Abbas. Use of fluid instabilities to enhance membrane performance: a review. *Desalination*, 136(1-3):255–262, 5 2001.

[9] Jean-Pierre Brun. *Procédés de séparation par membranes*. Elsevier Masson, 1 1989.

[10] Toshikatsu Sata. *Ion Exchange Membranes*. Royal Society of Chemistry, 10 2007.

[11] Nikolay Voutchkov. *Desalination Engineering: Planning and Design*. McGraw Hill Professional, 12 2012.

[12] Lawrence K. Wang, Jia-Ping Chen, Yung-Tse Hung, and Nazih K. Shammas. *Membrane and Desalination Technologies*. 1 2011.

[13] H Strathmann. *Ion-Exchange Membrane Separation Processes*. Elsevier, 1 2004.

[14] Eric M. V. Hoek and Volodymyr V. Tarabara. *Encyclopedia of Membrane Science and Technology, 3 Volume Set*. Wiley, 10 2013.

[15] Yoshinobu Tanaka. *Ion Exchange Membranes*. Elsevier Science, 1 2015.

[16] Andréa Moura Bernardes, Marco Antônio Siqueira Rodrigues, and Jane Zoppas Ferreira. *Electrodialysis and Water Reuse*. Springer Science Business Media, 8 2013.

[17] Norman N Li, Anthony G. Fane, W. S. Winston Ho, and Takeshi Matsuura. *Advanced Membrane Technology and Applications*. John Wiley Sons, 9 2011.

[18] Taner Yonar. *Electrodialysis*. BoD – Books on Demand, 12 2020.

[19] Luigi Gurreri, Alessandro Tamburini, and Giorgio Micale. Electromembrane Processes: Experiments and Modelling. *Membranes*, 11(2):149, 2 2021.

[20] Lucía Alvarado and Aicheng Chen. Electrodeionization: Principles, Strategies and Applications. *Electrochimica Acta*, 132:583–597, 6 2014.

[21] William V. Collentro. *Pharmaceutical Water: System Design, Operation, and Validation*. 9 1998.

[22] Nicholas P Cheremisinoff. *Handbook of Water and Wastewater Treatment Technologies*. Butterworth-Heinemann, 1 2002.

[23] Anthony M. Wachinski. *Environmental Ion Exchange*. CRC Press, 10 2016.

[24] Andrei A. Zagorodni. *Ion Exchange Materials: Properties and Applications*. Elsevier, 11 2006.

[25] Anthony M. Wachinski. *Ion Exchange Treatment for Water*. 1 2006.

[26] F.C. Nachod. *Ion Exchange*. Elsevier, 12 2012.

[27] Jerry R. Perrich. *Activated Carbon Adsorption for Wastewater Treatment.* CRC Press, 11 2017.

[28] W. Kelley Thomas and Barry Crittenden. *Adsorption technology and design.* 1 1998.

[29] Kerry J. Howe, David W. Hand, John C. Crittenden, R. Rhodes Trussell, and George Tchobanoglous. *Principles of Water Treatment.* John Wiley Sons, 11 2012.

[30] Ferhan Cecen and Özgür Aktas. *Activated Carbon for Water and Wastewater Treatment.* John Wiley Sons, 9 2011.

[31] Samuel Denton Faust and Osman M. Aly. *Chemistry of Water Treatment.* Butterworth-Heinemann, 1 1983.

[32] Chi Tien. *Introduction to Adsorption.* Elsevier, 11 2018.

[33] Christopher J. Corwin and R. Scott Summers. Scaling Trace Organic Contaminant Adsorption Capacity by Granular Activated Carbon. *Environmental Science Technology*, 44(14):5403–5408, 6 2010.

[34] V. Dean Adams. *Water and Wastewater Examination Manual.* CRC-Press, 8 1990.

[35] Amel KAMOUN, Mohamed Moncef CHAABOUNI, and Hassine Ferid AYEDI. Plans d'expériences et traitements de surface méthodologie des surfaces de réponses (msr). *Techniques de l'ingénieur Traitements de surface des métaux : contexte et gestion environnementale*, base documentaire : TIB502DUO.(ref. article : m1429), 2011.

[36] Décret exécutif n 06-14 du 20 Rabie El Aouel 1427 correspondant au 19 avril 2006. *JOURNAL OFFICIEL DE LA REPUBLIQUE ALGERIENNE N 26*, 06-14, 4 2006.

[37] P. Ravikumar, K. L. Prakash, and R. K. Somashekar. Evaluation of water quality using geochemical modeling in the Bellary Nala Command area, Belgaum district, Karnataka State, India. *Carbonates and Evaporites*, 28(3):365–381, 2 2013.

[38] Douglas M. Ruthven. *Principles of Adsorption and Adsorption Processes.* John Wiley Sons, 6 1984.

[39] Ehsan Mohammad-Pajooh, Ariel E. Turcios, Graham Cuff, Dirk Weichgrebe, Karl-Heinz Rosenwinkel, M. D. Vedenyapina, and L. R. Sharifullina. Removal of inert COD and trace metals from stabilized landfill leachate by granular activated carbon (GAC) adsorption. *Journal of Environmental Management*, 228:189–196, 12 2018.

[40] Wen Xing, Huu Hao Ngo, S. H. Kim, Wei Guo, and P. Hagare. Adsorption and bioadsorption of granular activated carbon (GAC) for dissolved organic carbon (DOC) removal in wastewater. *Bioresource Technology*, 99(18):8674–8678, 12 2008.

[41] Ananda J. Jadhav and Vimal Chandra Srivastava. Adsorbed solution theory based modeling of binary adsorption of nitrobenzene, aniline and phenol onto granulated activated carbon. *Chemical Engineering Journal*, 229:450–459, 8 2013.

[42] Takashi Asano. *Water Reuse*. McGraw Hill Professional, 1 2007.

[43] Xiaomeng Wang, Ning Li, Jianye Li, Junjun Feng, Zhun Ma, Yuting Xu, Yongchao Sun, Dongmei Xu, Jing Wang, Xueli Gao, and Jun Gao. Fluoride removal from secondary effluent of the graphite industry using electrodialysis: Optimization with response surface methodology. *Frontiers of Environmental Science Engineering*, 13(4), 5 2019.

[44] LAKEHAL AICHA. *Influence de la nature des ions et des résines échangeuses sur les performances de l'électrodéionisation/ Application aux métaux lourds pour la dépollution et aux eaux naturelles pour la déminéralisation.* PhD thesis, UNIVERSITE EL HADJ LAKHDAR-BATNA, 2011.

[45] Oumeima Souilah, D.E. Akretche, and M. Amara. Water reuse of an industrial effluent by means of electrodeionisation. *Desalination*, 167:49–54, 8 2004.

[46] Fazel Zahakifar, A.R. Keshtkar, Ehsan Zamani Souderjani, and Mohammad Ali Moosavian. Use of response surface methodology for optimization of thorium(IV) removal from aqueous solutions by electrodeionization (EDI). *Progress in Nuclear Energy*, 124:103335, 6 2020.

[47] Youcef Sedkaoui, Anthony Szymczyk, Hakim Lounici, and Omar Arous. A new lateral method for characterizing the electrical conductivity of ion-exchange membranes. *Journal of Membrane Science*, 507:34–42, 6 2016.

Appendix A

Additionals information

A.1 Membrane properties [47]

TABLE 1 Characteristics of the membranes*

membrane	concentration of fixed-ion mg·equiv.·cm^{-3}	concentration of co-ion mg·equiv.·cm^{-3}	thickness cm	specific resistance Ω·cm	self-diffusion constant of Cl^- cm^2·sec^{-1}	salt diffusion constant cm^2·sec^{-1}
CMV	1.5	1.37×10^{-4}**	0.13×10^{-2}	190~230	5×10^{-8}	$<1\times10^{-9}$
AMV	1.5	10^{-4}	0.14×10^{-2}	280~320	1×10^{-8}***	$<1\times10^{-9}$

* Selemion membranes of Asahi Glass Co., Ltd.

** Measured by ^{36}Cl concentration in the wet membrane which is in equilibrium with 0.01 M NaCl aqueous solution containing ^{36}Cl.

*** The self diffusion of Cl^- for anion exchange membrane is controlled by the diffusion across the membrane-solution interface, whereas it is controlled by the diffusion through the membrane itself for cation exchange membrane.

	AMX	**CMX**
Manufacturer	Tokuyama Soda (Japan)	
Type	Homogeneous	
Thickness (mm)[a]	0.14	0.17
Specific resistance (Ω cm²) in 0.5 M NaCl solution[a]	2.4	3.0
Ion exchange capacity (mmol equiv/g)	1.30 ± 0.05[b]	1.65[c]
Water content (g H_2O/g dry membrane)	0.10–0.14[b]	0.275[c]
Membrane density (g/cm^3)	1.10[b]	1.19[c]

Figure A.1: Main properties of AMX and CMX membranes.

Appendix B

Algorithms.

B.1 Algorithm of Langmuir model fit

```
% Define the input data as column vectors
c = [40.2; 9.28; 4.28; 2.88];
q = [20.3; 7.79; 5.98; 4.76];
% Define the Langmuir adsorption model as a function
langmuir = @(theta, c) (theta(1) * theta(2) * c(:)) ./ (1 + theta(1) * c(:));
% Set the initial guess for k and Qmax
theta0 = [0.01, max(q)];
% Call lsqcurvefit to fit the model to the data
options = optimoptions(@lsqcurvefit, 'Display', 'iter');
params = lsqcurvefit(langmuir, theta0, c, q, [], [], options);
% Extract the fitted values of k and Qmax
k_fit = params(1);
Qmax_fit = params(2);
% Generate a plot of the Langmuir model fit
c_fit = linspace(min(c), max(c), 100);
q_fit = langmuir([k_fit, Qmax_fit], c_fit);
plot(c, q, 'o', c_fit, q_fit);
title('Langmuir Adsorption Model Fit');
xlabel('Concentration (mg /L)');
ylabel('Quantity adsorbed (mg /g)');
legend('Experimental Data', 'Model Fit', 'Location', 'NorthWest');
```

B.2 Algorithm of Freundlich model fit

```
% Define the input data as column vectors
c = [40.2; 9.28; 4.28; 2.88];
q = [20.3; 7.79; 5.98; 4.76];

% Define the Freundlich adsorption model as a function
freundlich = @(theta, c) theta(1) * c.^theta(2);

% Set the initial guess for Kf and n
theta0 = [0, 0];

% Call lsqcurvefit to fit the model to the data
options = optimoptions(@lsqcurvefit, 'Display', 'iter');
params = lsqcurvefit(@(theta, c) freundlich(theta, c), theta0, c, q, [], [], options)

% Extract the fitted values of Kf and n
Kf_fit = params(1);
n_fit = params(2);

% Calculate the coefficient of determination R^2 = corr^2
R = corrcoef(c, q);
corr = R(1, 2);

% Generate a plot of the Freundlich model fit
c_fit = linspace(min(c), max(c), 100);
q_fit = freundlich([Kf_fit, n_fit], c_fit);
plot(c, q, 'o', c_fit, q_fit);
title('Freundlich Adsorption Model Fit');
xlabel('Concentration (mg/L)');
ylabel('Quantity adsorbed (mg/g)');
legend('Experimental Data', 'Model Fit', 'Location', 'NorthWest');
```

B.3 Algorithm of dynamic adsorption model fit

```
% Experimental data
TOC_mg/L = [0; 10.68; 14.68; 22.68; 24.68; 26.68; 34.68; 58.68; 78.68; 85.12; 91.08];
volume_l = [0; 1.5; 1.8; 2.4; 3.5; 3.8; 4.1; 6.1; 6.6; 6.9; 7.2];
% Constants
M = 15;
C_0 = 91.08;
Q = 0.0004901960784;
% Define the Thomas equation
thomas_eqn = @(x, V) C_0./(1 + exp(x(1)*(Q*(x(2)*M - C_0*V))));
% Initial guess for the parameters
x0 = [1, 1];
% Perform curve fitting
x = lsqcurvefit(thomas_eqn, x0, volume_l, TOC_ppm);
% Extract the constants
k_1 = x(1);
Q_0 = x(2);
% Display the constants
disp(['k_1 = ' num2str(k_1)]);
disp(['Q_0 = ' num2str(Q_0)]);
% Plot the fit curve
V_fit = linspace(0, max(volume_l), 100);
TOC_ppm_fit = thomas_eqn(x, V_fit);
figure;
plot(volume_l, TOC_ppm, 'ro', 'MarkerSize', 5);
hold on;
plot(V_fit, TOC_ppm_fit, 'b-', 'LineWidth', 1);
xlabel('Volume (l)');
ylabel('TOC (mg/L)');
legend('Experimental Data', 'Fit Curve');
title('Adsorption on Granulated Carbon (Thomas Equation)');
```